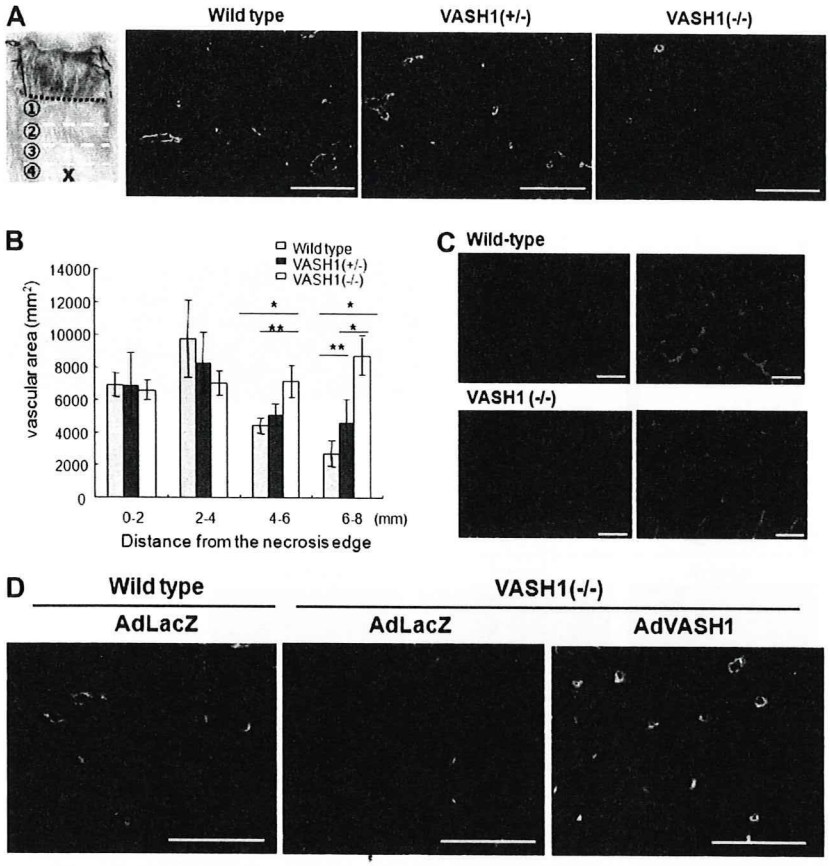

Figure 6. Vascular distribution in the skin flap of *VASH1* knockout mice. *VASH1* knockout mice were applied to the model of subcutaneous angiogenesis. (A) Immunostaining of CD31 (red) and αSMA (green) in the area 6 to 8 mm from the necrotic edge is shown. Scale bars are 200 μm. (B) The vascular area was determined from 5 different fields in each area. Data are expressed as the means and SDs; $^{*}P < .01$, $^{**}P < .05$. (C) Lectin staining (green) shows the perfusion of new vessels in the area 6 to 8 mm from the necrotic edge. The same section was immunostained for CD31 (red). Scale bars are 200 μm. (D) Adenoviral-mediated gene transfer was performed to supplement the deficient protein in *VASH1* knockout mice. AdLacZ was use as the control. Immunostaining of CD31 (red) and αSMA (green) in the indicated area of the skin flap is shown. Scale bars are 200 μm.

sensitive at the sprouting front where endogenous VASH2 should be enriched (Figure 7A,B). Importantly, the extent of MNC infiltration in the sprouting front was not altered in *VASH2*$^{-/-}$ mice (Figure 7C). Again, supplementation of the deficient proteins by adenoviral-mediated gene transfer normalized the abnormal angiogenesis patterns in *VASH2* knockout mice (Figure 7D).

Discussion

We characterized the roles of the 2 members of the vasohibin family in the regulation of angiogenesis with the use of a mouse model of subcutaneous angiogenesis. The spatiotemporal expression pattern and substantial effects of these 2 molecules indicate that VASH1 and VASH2 control the promotion and termination of angiogenesis in a complementary manner.

The expression of endogenous VASH1 was augmented in nonproliferating ECs in the termination zone of postnatal angiogenesis. This VASH1 in the termination zone should be involved in halting angiogenesis, because angiogenesis persisted in the termination zone in *VASH1* knockout mice in a gene-dosage manner. This result also implies that endogenous VASH1 is not a principal regulator limiting the sprouting. However, when applied exogenously, VASH1 can inhibit angiogenesis at the sprouting front where endogenous VASH1 is scarce. In addition, exogenous VASH1 exhibits little effect, if any, in the termination zone where endogenous VASH1 is present. Accordingly, the present results show the distinctive acting points of endogenous and exogenous VASH1 and further support the legitimacy of using exogenous VASH1 as an antiangiogenic treatment.

Endogenous VASH2, in contrast, was expressed mainly by infiltrating bone marrow–derived MNCs at the sprouting front in our model. The present result contrasts with our previous observation about VASH2 expression in ECs of developing embryos without obvious MNC infiltration.[16] About the expression of VASH2 in MNCs, monocytic THP-1 cells were found to express VASH2 more abundantly than ECs in culture. Hence, MNCs can be the main source of VASH2 when they infiltrate.

Bone marrow–derived cells, including endothelial progenitor cells (EPCs), contribute to postnatal angiogenesis.[22] However, we could hardly detect the integration of bone marrow–derived cells in the neo-vessels in our model, indicating that EPCs might not play a major role in our model. What we observed was that most of the bone marrow–derived cells infiltrated in the sprouting front were MNCs. It is described that bone marrow–derived MNCs stimulate angiogenesis by producing angiogenic factors, including VEGF and several matrix metalloproteinases.[23,24] Along these lines, we propose that VASH2 produced by bone marrow–derived MNCs takes part in the promotion of postnatal angiogenesis, because angiogenesis at the sprouting front is significantly impaired in *VASH2* knockout mice even in the presence of MNC infiltration. Appropriately, exogenous VASH2 inhibited the termination of angiogenesis in the termination zone where endogenous VASH2 staining was faint.

We previously reported that, when applied exogenously, VASH-2 exhibited the antiangiogenic activity in the mouse cornea.[16] However, to our surprise, the present study rather indicated the proangiogenic activity of VASH2. Amino acid sequence of VASH2 is 52.5% homologous to that of VASH1 in humans, and 51.9% homologous in mice.[16] We therefore hypothesize the role of

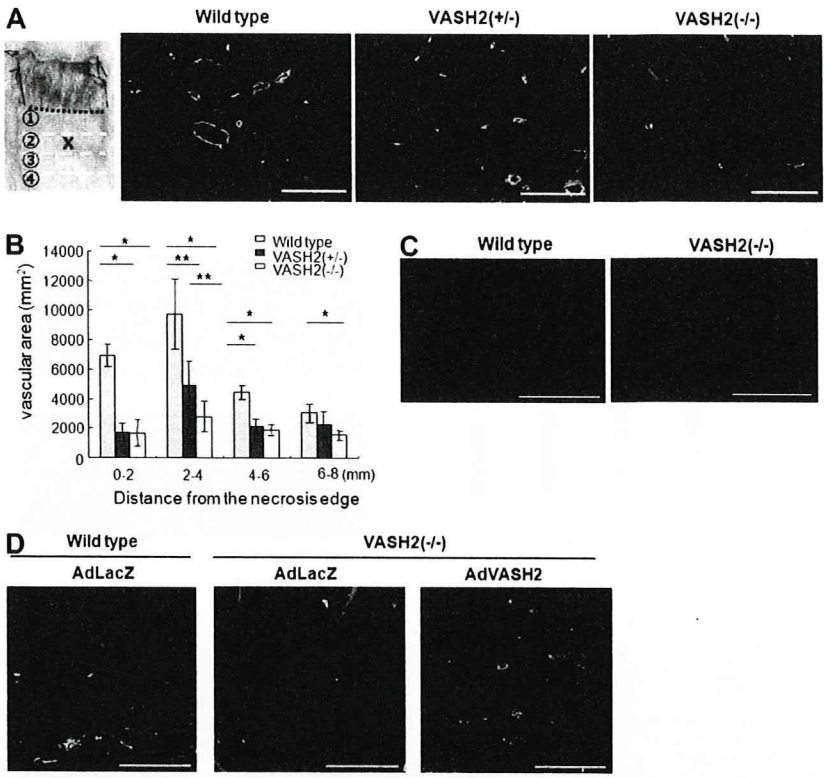

Figure 7. Vascular distribution in the skin flap of *VASH2* knockout mice. *VASH2* knockout mice were applied to the model of subcutaneous angiogenesis. (A) Immunostaining of CD31 (red) and αSMA (green) in the area 2 to 4 mm from the necrotic edge is shown. Scale bars are 200 μm. (B) The vascular area was determined from 5 different fields in each area. Data are expressed as the means and SDs; $^{*}P < .01$, $^{**}P < .05$. (C) Immunostaining of CD11b (red) in the area 0 to 2 mm from the necrotic edge is shown in wild-type and *VASH2*$^{-/-}$ mice. Scale bars are 200 μm. (D) Adenoviral-mediated gene transfer was performed to supplement the deficient protein in *VASH2* knockout mice. AdLacZ was use as the control. Immunostaining of CD31 (red) and αSMA (green) in the indicated area of the skin flap is shown. Scale bars are 200 μm.

VASH2 as follows. On the analogy to angiopoietin-1 and angiopoietin-2, VASH1 and VASH2 may share the same receptor. VASH2 is a weak agonist and antagonizes VASH1 in a certain condition, although the receptor for the VASH family is not yet identified. We are currently testing this hypothesis.

There are several endogenous angiogenesis inhibitors in the body, but it is still not clear why the body needs so many angiogenesis inhibitors. Systematic analysis to show how these endogenous angiogenesis inhibitors orchestrate the control of angiogenesis is lacking. Delta-like 4 (Dll4) is the ligand of Notch1, which determines the arterial specification of ECs.[25,26] However, recent evidence indicates that ECs at the sprouting tip express Dll4 and that this Dll4 negatively regulates the formation of appropriate numbers of sprouting tips.[27-31] Therefore, Dll4 and VASH1 are 2 inhibitors that are expressed in ECs, but the apparent difference between VASH1 and Dll4 is their temporal expression patterns. Dll4 is selectively expressed in tip cells, whereas VASH1 is expressed in ECs in the termination zone. Hence, VASH1 and Dll4 are expressed in different phases of angiogenesis and should negatively tune this phenomenon distinctively. It is described that inactivation of Dll4 increases sprouting microvessels without proper blood perfusion.[32,33] Importantly, increased numbers of microvessels in the termination zone of *VASH1*$^{-/-}$ mice were patent and maintained blood perfusion. This difference in blood perfusion further proposes the distinctive roles of VASH1 and Dll4 in the regulation of angiogenesis.

In summary, the vasohibin family members, VASH1 and VASH2, participate in the regulation of angiogenesis in a previously unrecognized manner. VASH1 is expressed in ECs in the termination zone to halt angiogenesis, whereas VASH2 is expressed mainly in infiltrating MNCs at the sprouting front to promote angiogenesis. Discovery of these molecules should provide novel approaches to both antiangiogenic and proangiogenic treatments. Further study is currently under way to clarify the underlying mechanism how VASH1 and VASH2 regulate angiogenesis in an opposed but complementary manner.

Acknowledgments

This work was supported by a Grant-in-Aid for Scientific Research on Priority Areas of the Japanese Ministry of Education, Science, Sports, and Culture from the Ministry of Education, Science, Sports, and Culture of Japan (contract grants 16022205 and 17014006), and by the 21st Century COE Program Special Research Grant "The Center for Innovative Therapeutic Development Towards the Conquest of Signal Transduction Diseases" from the Ministry of Education, Science, Sports, and Culture of Japan.

Authorship

Contribution: H.K. performed research and wrote the paper; H.M. and Y.S. prepared the knockout mice; M.K. performed transfection to MS1 cells; K.W. performed analysis of the intracellular localization; H.S. and H.O. prepared antibodies; T.F. performed electron microscopy; T.S. designed the research; and Y.S. designed the research and wrote the paper.

Conflict-of-interest disclosure: The authors declare no competing financial interests.

Correspondence: Yasufumi Sato, Department of Vascular Biology, Institute of Development, Aging and Cancer, Tohoku University, 4-1 Seiryo-machi, Aoba-ku, Sendai 980-8575, Japan; e-mail: y-sato@idac.tohoku.ac.jp.

References

1. Adams RH, Alitalo K. Molecular regulation of angiogenesis and lymphangiogenesis. Nat Rev Mol Cell Biol. 2007;8:464-478.
2. Sato Y. Update on endogenous inhibitors of angiogenesis. Endothelium. 2006;13:147-155.
3. Dawson DW, Volpert OV, Gillis P, Crawford SE, et al. Pigment epithelium-derived factor: a potent inhibitor of angiogenesis. Science. 1999;285:245-248.
4. Renno RZ, Youssri AI, Michaud N, Gragoudas ES, Miller JW. Expression of pigment epithelium-derived factor in experimental choroidal neovascularization. Invest Ophthalmol Vis Sci. 2002;43:1574-1580.
5. Hiraki Y, Inoue H, Iyama K, et al. Identification of chondromodulin I as a novel endothelial cell growth inhibitor. Purification and its localization in the avascular zone of epiphyseal cartilage. J Biol Chem. 1997;272:32419-32426.
6. Yoshioka M, Yuasa S, Matsumura K, et al. Chondromodulin-I maintains cardiac valvular function by preventing angiogenesis. Nat Med. 2006;12:1151-1159.
7. Zhang M, Volpert O, Shi YH, Bouck N. Maspin is an angiogenesis inhibitor. Nat Med. 2000;6:196-199.
8. Maass N, Nagasaki K, Ziebart M, Mundhenke C, Jonat W. Expression and regulation of tumor suppressor gene maspin in breast cancer. Clin. Breast Cancer. 2002;3:281-287.
9. Kopp HG, Hooper AT, Broekman MJ, et al. Thrombospondins deployed by thrombopoietic cells determine angiogenic switch and extent of revascularization. J Clin Invest. 2006;116:3277-3291.
10. Kalluri R. Basement membranes: structure, assembly and role in tumour angiogenesis. Nat Rev Cancer. 2003;3:422-433.
11. Watanabe K, Hasegawa Y, Yamashita H, et al. Vasohibin as an endothelium-derived negative feedback regulator of angiogenesis. J Clin Invest. 2004;114:884-886.
12. Shimizu K, Watanabe K, Yamashita H, et al. Gene regulation of a novel angiogenesis inhibitor, vasohibin, in endothelial cells. Biochem Biophys Res Commun. 2005;327:700-7006.
13. Sonoda H, Ohta H, Watanabe K, Yamashita H, Kimura H, Sato Y. Multiple processing forms and their biological activities of a novel angiogenesis inhibitor vasohibin. Biochem Biophys Res Commun. 2006;342:640-646.
14. Shen JK, Yang XR, Sato Y, Campochiaro PA. Vasohibin is up-regulated by VEGF in the retina and suppresses VEGF receptor 2 and retinal neovascularization. FASEB J. 2006;20:723-725.
15. Yamashita H, Abe M, Watanabe K, et al. Vasohibin prevents arterial neointimal formation through angiogenesis inhibition. Biochem Biophys Res Commun. 2006;345:919-925.
16. Shibuya T, Watanabe K, Yamashita H, et al. Isolation of vasohibin-2 as a sole homologue of VEGF-inducible endothelium-derived angiogenesis inhibitor vasohibin: a comparative study on their expressions. Arterioscler Thromb Vasc Biol. 2006;26:1051-1057.
17. Sato Y, Sonoda H. The vasohibin family: a negative regulatory system of angiogenesis genetically programmed in endothelial cells. Arterioscler Thromb Vasc Biol. 2007;27:37-41.
18. Tepper OM, Capla JM, Galiano RD, et al. Adult vasculogenesis occurs through in situ recruitment, proliferation, and tubulization of circulating bone marrow-derived cells. Blood. 2005;105:1068-1077.
19. Oike Y, Akao M, Yasunaga K, et al. Angiopoietin-related growth factor antagonizes obesity and insulin resistance. Nat Med. 2005;11:400-408.
20. Yamazaki D, Suetsugu S, Miki H, et al. WAVE2 is required for directed cell migration and cardiovascular development. Nature. 2003;424:452-456.
21. Namba K, Abe M, Saito S, et al. Indispensable role of the transcription factor PEBP2/CBF in angiogenic activity of a murine endothelial cell MSS31. Oncogene. 2000;19:106-114.
22. Rabbany SY, Heissig B, Hattori K, Rafii S. Molecular pathways regulating mobilization of marrow-derived stem cells for tissue revascularization. Trends Mol Med. 2003;9:109-117.
23. Barbera-Guillem E, Nyhus JK, Wolford CC, Friece CR, Sampsel JW. Vascular endothelial growth factor secretion by tumor-infiltrating macrophages essentially supports tumor angiogenesis, and IgG immune complexes potentiate the process. Cancer Res. 2002;62:7042-7049.
24. Cho CH, Koh YJ, Han J, et al. Angiogenic role of LYVE-1-positive macrophages in adipose tissue. Circ Res. 2007;100:e47-57.
25. Shutter JR, Scully S, Fan W, et al. Dll4, a novel Notch ligand expressed in arterial endothelium. Genes Dev. 2000;14:1313-1318.
26. Duarte A, Hirashima M, Benedito R, et al. Dosage-sensitive requirement for mouse Dll4 in artery development. Genes Dev. 2004;18:2474-2478.
27. Williams CK, Li JL, Murga M, Harris AL, Tosato G. Up-regulation of the Notch ligand Delta-like 4 inhibits VEGF-induced endothelial cell function. Blood. 2006;107:931-939.
28. Hellstrom M, Phng LK, Hofmann JJ, et al. Dll4 signalling through Notch1 regulates formation of tip cells during angiogenesis. Nature. 2007;445:776-780.
29. Siekmann AF, Lawson ND. Notch signalling limits angiogenic cell behaviour in developing zebrafish arteries. Nature. 2007;445:781-784.
30. Leslie JD, Ariza-McNaughton L, Bermange AL, McAdow R, Johnson SL, Lewis J. Endothelial signaling by the Notch ligand Delta-like 4 restricts angiogenesis. Development. 2007;134:839-844.
31. Lobov IB, Renard RA, Papadopoulos NJ, et al. Delta-like ligand 4 (Dll4) is induced by VEGF as a negative regulator of angiogenic sprouting. Proc Natl Acad Sci U S A. 2007;104:3219-3224.
32. Noguera-Troise I, Daly C, Papadopoulos NJ, et al. Blockade of Dll4 inhibits tumour growth by promoting nonproductive angiogenesis. Nature. 2006;444:1032-1037.
33. Ridgway J, Zhang G, Wu Y, et al. Inhibition of Dll4 signalling inhibits tumour growth by deregulating angiogenesis. Nature. 2006;444:1083-1087.

J. Biochem. 2009;145(5)653–659
doi:10.1093/jb/mvp021

Induction and Expression of Anti-Angiogenic Vasohibins in the Hematopoietic Stem/Progenitor Cell Population

Hisamichi Naito[1], Hiroyasu Kidoya[1], Yasufumi Sato[2] and Nobuyuki Takakura[1,*]

[1]Department of Signal Transduction, Research Institute for Microbial Diseases, Osaka University, 3-1 Yamada-oka, Suita-shi, Osaka 565-0871, Japan; and [2]Department of Vascular Biology, Institute of Development, Aging, and Cancer, Tohoku University, 4-1 Seiryo-machi, Aoba-ku, Sendai 980-8575, Japan

Received January 8, 2009; accepted January 23, 2009; published online January 29, 2009

Haematopoiesis and blood vessel formation are closely associated, with several molecules employed by both systems. Recently, vasohibin-1 (VASH1), an endothelium-derived negative feedback regulator of angiogenesis, has been isolated and characterized. VASH1 is induced by VEGF or bFGF in endothelial cells (ECs) and inhibits their proliferation and migration. However, there are no data on the induction and expression of VASH1 in haematopoietic cells (HCs). Here, we show that the haematopoietic stem cell (HSC) population, but not haematopoietic progenitors (HPs) or mature HCs from adult bone marrow (BM) constitutively express VASH1. However, HPs, but not HSCs, can be induced to express VASH1 after BM suppression by 5-FU. Knock-down of the *VASH1* gene in VASH1$^+$ leukaemia cells induced cell proliferation. These results suggest a role for VASH1 in negative feedback regulation of HP proliferation during recovery following BM ablation.

Key words: 5-FU, bone marrow ablation, haematopoietic progenitor cells, haematopoietic stem cell, vasohibin.

Abbreviations: bFGF, basic fibroblast growth factor; BM, bone marrow; EC, endothelial cell; HC, haematopoietic cell; HP, haematopoietic progenitor; HSC, haematopoietic stem cell; VASH1, vasohibin-1; VEGF, vascular endothelial growth factor.

The haematopoietic and vascular systems are closely related in several respects. It has been suggested that haematopoietic cells (HCs) and endothelial cells (ECs) arise from a common progenitor during development, the so-called haemangioblast (*1*) or hemogenic angioblast (*2*), which originates from mesodermal cells. In addition, after the development of haematopoietic stem cells (HSCs) and ECs, the latter supports the differentiation, proliferation and survival of the former, which themselves support angiogenesis (*3–10*). Moreover, it has been reported that erythropoietin, originally identified as a haematopoietic cytokine, also induces proliferation of ECs (*11*), suggesting that there are several factors commonly utilized in vascular development and haematopoiesis.

Recently, a novel anti-angiogenic factor, vasohibin-1 (VASH1), has been isolated from human umbilical vein endothelial cells (HUVECs) (*12*). VASH1 is upregulated by vascular endothelial growth factor (VEGF) in HUVECs and has been suggested to act as a negative feedback regulator of VEGF and basic fibroblast growth factor (bFGF) signalling in HUVECs. VASH1 is widely conserved among species (*13*) and is present in multiple processing forms (*14*), and it has been reported that alternative splicing of the VASH1 pre-mRNA transcript generates a potent anti-angiogenic protein (*15*). However, in mice, alternatively spliced forms of VASH1 have not been isolated. One VASH1 paralogue, termed vasohibin-2 (VASH2), with anti-angiogenic activity in mammals, has also been isolated recently (*16*). VASH1 is upregulated in retina upon stimulation with VEGF and suppresses retinal neovascularization in mice with ischemic retinopathy (*17*). VASH1 expression has been observed in ECs of adventitial microvessels in atherosclerotic lesions, where it inhibits adventitial angiogenesis and neointimal formation after cuff placement on the mouse femoral artery (*18*). Moreover, VASH1 is selectively expressed on vascular EC in both cyclic endometria and endometrial carcinomas and suppresses tumour growth and angiogenesis in a mouse xenograft tumour model (*19*). Taken together, these data suggest that VASH1 is a candidate target molecule for manipulating tumour angiogenesis.

While the unique function of VASH1 as a negative feedback regulator of angiogenesis has been extensively studied, its expression in cell lineages other than ECs has not been documented. On the basis of the hypothesis that the haematopoietic and vascular systems utilize similar molecules, here, we investigated the expression of VASH1 in several fractions of normal HCs in the bone marrow (BM) as well as in leukaemic cells and assessed the mechanisms regulating HC VASH1 expression.

MATERIALS AND METHODS

Mice—C57BL/6 mice were purchased from SLC (Shizuoka, Japan). All animal studies were approved by

*To whom correspondence should be addressed. Tel: +81-6-6879-8316, Fax: +81-6-6879-8314,
E-mail: ntakaku@biken.osaka-u.ac.jp

the Animal Care Committee of Osaka University. For BM ablation studies, 10-week-old mice were treated with a single-tail vein injection of 5-FU (Kyowa Hakko Kogyo Co., Ltd, Tokyo, Japan; 150 mg/kg body weight). The mouse model of hind limb ischemia was as described previously (*3*).

Cell Preparation and Flow Cytometry—Cell preparation from the hind limb, BM and peripheral blood was carried out as previously reported (*3*). The cell-staining procedure for flow cytometry was as described previously (*3*) using anti-CD31, -CD45, -c-kit, -Sca-1 and anti-lineage (a mixture of ter119, Gr-1, Mac-1, B220, CD4 and CD8) monoclonal antibodies (mAbs; all from Pharmingen). All mAbs were purified and conjugated with either FITC or PE (phycoerythrin) or biotin. Biotinylated antibodies were visualized with PE-conjugated streptavidin or APC-conjugated streptavidin (Pharmingen). The stained cells were analysed and sorted by JSAN (Bay Bioscience, Kobe, Japan). For the procedures involving SP cells, Hoechst dye was used as previously described (*20, 21*). BMMNCs were resuspended at 1×10^6 cells/ml and incubated with Hoechst 33342 (5 μg/ml) for 90 min at 37°C. Cells were then washed and analysed by JSAN (Bay Bioscience).

Quantitative Real-Time Reverse Transcription PCR (qRT–PCR) Analysis—Extraction of total RNA and qRT–PCR was performed as previously reported (*22*). Levels of specific amplified cDNA were normalized to *glyceraldehyde-3-phosphate dehydrogenase* (*GAPDH*) housekeeping gene levels. Primers used in this experiment were as follows: mouse *VASH1* (corresponding to human *VASH1A*, sense 5′-CAT CAG GGA GCT GCA GTA CA-3′, anti-sense 5′-GAT CAC AGC TTC CAG GCA TT-3′), human *VASH1A* (sense 5′-GCT GCA GTA CAA TCA CAC AGG-3′, anti-sense 5′-AGG TAA ATT CCC AGG ATC ACG-3′), human *VASH1B* (sense 5′-AAG CTG TGC AGC GTC ACA TC-3′, anti-sense 5′-ACT TTC AGA GCA GGA AGC TGA-3′) (*15*), mouse *GAPDH* (sense 5′-TGG CAA AGT GGA GAT TGT TGC C-3′, anti-sense 5′-AAG ATG GTG ATG GGC TTC CCG-3′), human *GAPDH* (sense 5′-GAA GGT GAA GGT CGG AGT C-3′ and anti-sense 5′-GAA GAT GGT GAT GGG ATT TC-3′).

Western Blotting Analysis—Methods for western blotting were previously described (*22*). Antibodies used in this experiment were anti-VASH1 (*12*) and anti-GAPDH (Chemicon, Temecula, CA).

Cell Lines—HUVECs were purchased from Kurabo (Osaka, Japan) and cultured in Humedia EG2 (Kurabo). For the induction analysis of VASH1A, HUVECs were starved for 12 h and stimulated with VEGF-A_{165} (10 ng/ml, PeproTech, Rocky Hill, NJ) for 12 h.

Human leukaemia cell lines (KG1a, HL60, THP-1, MOLT-4, SKW3, BALL-1 and NALM6) as indicated in Fig. 4A were provided by the Riken Bioresource Center (Tsukuba, Japan) and the Cell Resource Center for Biomedical Research, Institute of Development, Aging and Cancer, Tohoku University.

RNAi and Transfection—Two Stealth™ RNAi duplexes were synthesized commercially by Invitrogen. Stealth RNAi duplexes with GC content similar to that of each test duplex were used as a negative control. Stealth™ RNAi #1 (5′-UCU GAU AUA GCG CUG CAC AGC UUC C-3′), Stealth™ RNAi #2 and Stealth™ RNAi #2 (5′-UUC CCU GAG AAG UAG GUC UUG AAG C-3′) were designed to target different coding regions of the human *Vash1* mRNA sequence. A BLAST (NCBI database) search was carried out to confirm that the targets of the two Stealth™ RNAi duplexes were exclusively in *Vash1*.

THP1 cells were seeded at 1×10^5 cells/ml, and transfection was accomplished using lipofectamine 2000 according to the manufacturer's instructions. For selecting transfected cells, each Stealth RNAi duplex was co-transfected with Block-iT Alexa Fluor Red Flurescent Oligo (Invitrogen) and 24 h later, positive cells were sorted by JSAN (Bay Bioscience) and cultured for growth assessment.

Statistical Analysis—All data are presented as mean ± SD. For statistical analysis, the statcel2 software package (OMS) was used with analysis of variance (ANOVA) performed on all data followed by Tukey–Kramer multiple comparison testing.

RESULTS

Expression of VASH1 in the HSC Population of Adult BM—Adult bone marrow (BM) cells were fractionated into a $Lin^-c\text{-}Kit^+Sca\text{-}1^+$ HSC-enriched population (KSL cells), a Lin^- haematopoietic progenitor (HP)-enriched population (Lin^- cells) and a differentiated HC (Lin^+ cells) population (Fig. 1A). qRT–PCR analysis (Fig. 1C) indicated that KSL cells express *VASH1* at higher levels than either Lin^- or Lin^+ cells. To further confirm the high level of *VASH1* expression in the HSC-enriched population, we identified HSCs by their ability to efflux Hoechst 33342 dye. This method defines an extremely small and haematopoietically potent subset of cells known as the side population (SP) (*20, 21*). As shown in Fig. 1B, ~0.1% of BM cells are in the SP cell fraction, as previously reported (*20*). Treatment with verapamil, an inhibitor of ATP-binding cassette transporter superfamily pumps, resulted in the complete disappearance of this population. qRT–PCR analysis (Fig. 1D) indicated that SP cells express *VASH1* at much higher levels than cells from the main population (MP) or from the S and G2/M stages of the cell cycle. Lin^+ cells seemed not to express *VASH1* (Fig. 1C); also lymphocytes, myeloid cells and erythroid cells from BM and mononuclear cells (MNCs) from peripheral blood do not express *VASH1* (Fig. 1F). Although ECs derived from hind limb muscle of adult mice do express *VASH1* at levels 5-fold those of the HSC population in BM (Fig. 1E); nonetheless, we concluded that among HCs, *VASH1* is preferentially expressed in the HSC population and not in HPs or mature HCs in the BM in the steady state. Since it has been reported that VASH1 expression was upregulated upon the stimulation with VEGF or bFGF using HUVECs (*12*), we tried to observe whether the expression of VASH1 is upregulated in freshly isolated ECs from hind limb muscle of adult mice as used in Fig. 1E. Perhaps, by the technical limitation using primary ECs, we could not observe the upregulation of *VASH1* on primary ECs under stimulation with VEGF or bFGF.

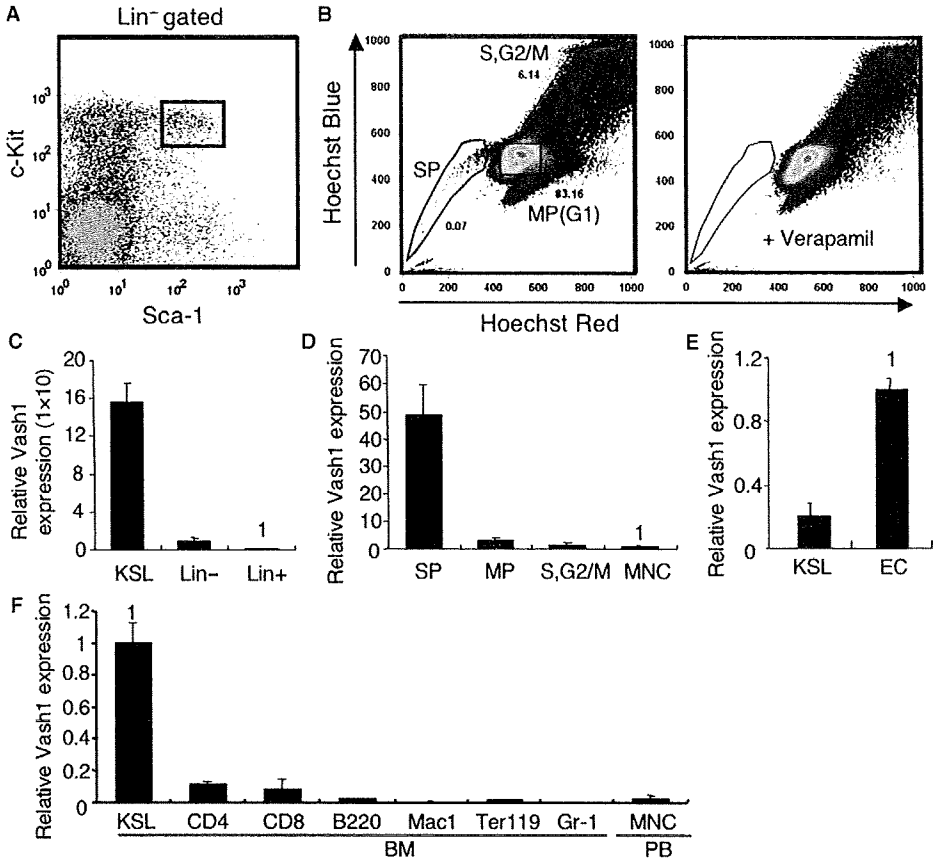

Fig. 1. **VASH1 expression in different haematopoietic lineages.** (A) Flow cytometric analysis of the HSC population. BM cells from 8-week-old mice were tested for the expression of Lin markers, c-Kit, Sca-1. Box indicates HSC population as Lin^{-}c-$Kit^{+}Sca\text{-}1^{+}$ cells. (B) Analysis of side population (SP) cells, main population (MP) cells and cells in the S, G2/M phase of the cell cycle from the BM of 8-week-old mice. The identification of SP cells was confirmed by their disappearance in the presence of Verapamil (right panel). (C–F) qRT–PCR for *VASH1* in several cells as indicated. Results (mean ± SD) are from three independently sorted sets of populations. (C) KSL HSC population, Lin^{-} haematopoietic progenitor-enriched population and Lin^{+} mature haematopoietic cells from BM of 8-week-old mice. (D) SP cells, MP cells and cells in S,G2/M from adult BM. Mononuclear cells (MNCs) from whole BM were also used for comparison. (E) Comparison of *VASH1* expression by KSL cells as indicated in (A) and ECs from hind limb muscle of 8-week-old mice defined as $CD31^{+}CD45^{-}$ cells. (F) Comparison of *VASH1* expression in KSL cells with adult BM cells positive for several lineage markers as indicated. MNCs from peripheral blood (PB) from the same mice were also used for comparison.

Ischaemia Does Not Induce VASH1 in HCs—In the murine femoral artery occlusion hind limb ischaemia model, the expression of VEGF and bFGF is increased (*23*). It has been reported that VASH1 expression is induced by VEGF or bFGF in ECs (*12*) and that several HCs including the HSC population migrate into ischemic tissue from BM to support angiogenesis (*8*). We reasoned that if regulatory mechanisms for VASH1 expression are similar in ECs and HCs, the latter may also express VASH1 in ischemic tissues. To test this, $CD31^{+}CD45^{-}$ ECs, $CD31^{-}CD45^{+}$ HCs and $CD31^{-}CD45^{-}$ non-EC/non-HCs were isolated from hind limb muscle in the normoxic or hypoxic condition and *VASH1* expression was examined (Fig. 2A). Although we could not succeed to induce *VASH1* expression in the culture of primary ECs as described earlier, we found that hypoxia-induced *VASH1* expression in ECs, but neither in HCs nor non-ECs/non-HCs (Fig. 2B). Moreover, ischaemia in the hind limb did not affect *VASH1* expression by HCs residing in the BM (data not shown). These findings suggested that the regulatory mechanisms controlling *VASH1* expression in HCs and ECs are different.

VASH1 Expression is Induced in HPs After BM Ablation by 5-FU—5-FU treatment in mice induces BM ablation as a result of killing the cycling HSCs and HPs. However, surviving HSCs and HPs undergo acute expansion to produce a number of mature HCs. We therefore analysed whether BM suppression with 5-FU affects *VASH1* expression. It is well known that although the HSC population is decreased in mice during the first few days after 5-FU (150 mg/kg) injection, the population of cycling HSCs and HPs increases dramatically 4–6 days thereafter (*24*). We therefore sorted KSL cells, Lin^{-} cells, and Lin^{+} cells from adult BM on day 7 after treatment with 5-FU (Fig. 2C and D). We found that *VASH1* expression in KSL cells and Lin^{+} cells was not affected by 5-FU injection, but that it was now induced in Lin^{-} HPs to a similar extent as present in KSL cells (Fig. 2D). This was also confirmed at the protein level (Fig. 2E).

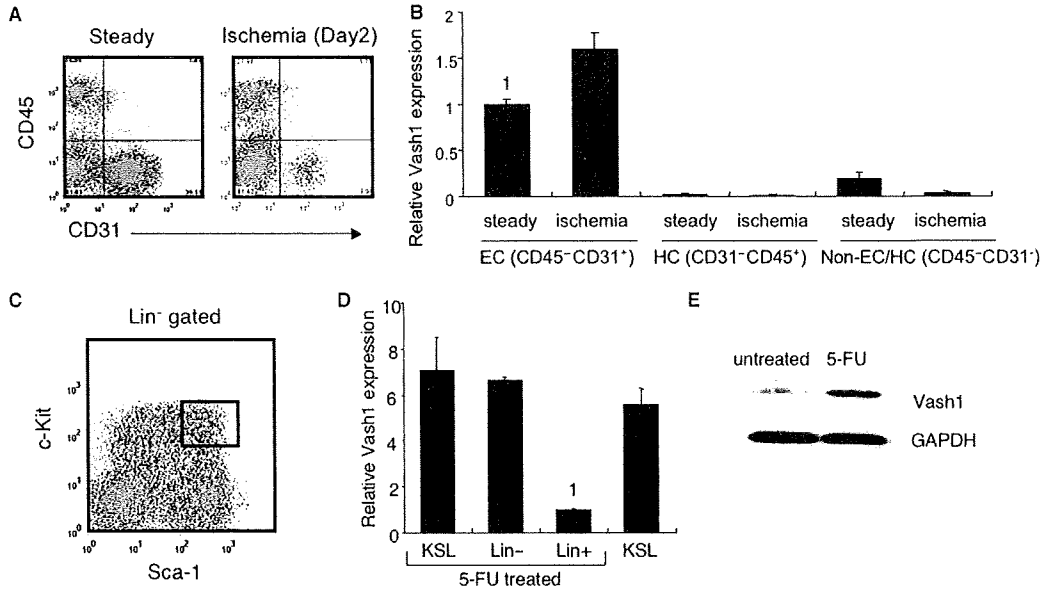

Fig. 2. **VASH1 expression on HCs in tissues under stress.** (A) Flow cytometric analysis of cells from hind limb muscle in the steady state and ischaemic state on the second day after femoral artery ligation. Cells were stained with CD31, an EC marker, and CD45, an HC marker. (B) qRT–PCR for *VASH1* expression in different cells sorted as shown in (A). Results (mean ± SD) are from three independently sorted sets of populations. C: BM cells from 10-week-old mice were isolated 7 days after systemic administration of 5-FU and tested for the expression of Lin markers, c-Kit, Sca-1 by flow cytometry. (D) qRT–PCR for levels of *VASH1* in KSL cells as shown in (C), Lin^- cells, and Lin^+ cells. KSL cells before 5-FU treatment are also used for comparison. (E) Western blotting for VASH1 expression. Lin^- haematopoietic progenitors from 10-week-old mice with or without 5-FU treatment were sorted and used for this analysis. GAPDH was used as an internal control.

VASH1 and VEGFR2 Expression in HPs After BM Ablation by 5-FU—It has been reported that HSCs and HPs express VEGFR2/Flk1, a receptor for VEGF, and that VEGF induces the expansion of $VEGFR2^+$ HPs (*25*). VEGF is upregulated after BM suppression (*26*). Moreover, knockdown of *VASH1* mRNA suggested that attenuation of VASH1 expression leads to a significant elevation in the level of *VEGFR2* mRNA in ECs (*17*). Therefore, it is possible that upregulated VASH1 in HPs suppresses VEGFR2 expression. Therefore, Lin^- BM HPs in the steady state and after 5-FU treatment were sorted into $VEGFR2^+$ and $VEGFR2^-$ populations (Fig. 3A) and their *VASH1* expression quantified. It was found that $VEGFR2^+$ cells expressed *VASH1* at higher levels than $VEGFR2^-$ cells in the steady state as well as after treatment with 5-FU (Fig. 3B). However, $VEGFR2^-$ cells from 5-FU-treated animals expressed more *VASH1* than those from controls (Fig. 3B). Moreover, cells very strongly positive for VEGFR2, which were present in controls, disappeared after 5-FU treatment (Fig. 3A, box in left panel). This suggests that VASH1 induction in $VEGFR2^{high}$ HPs after 5-FU treatment may attenuate the expression of VEGFR2, which may shift $VEGFR2^{high}$ cells to $VEGFR2^{low/-}$ cells.

Attenuation of Vash1 Expression Induces Proliferation of Leukaemia Cells—To seek models for understanding the role of VASH1 induction in HPs after BM ablation, we searched for VASH1-expressing HC lines. Of three human acute myeloblastic leukaemia (AML) cell lines, two (KG1a and THP1) strongly expressed *VASH1A*, but none of four acute lymphoid leukaemia (ALL) cell lines did so (Fig. 4A and B). In this experiment, we used

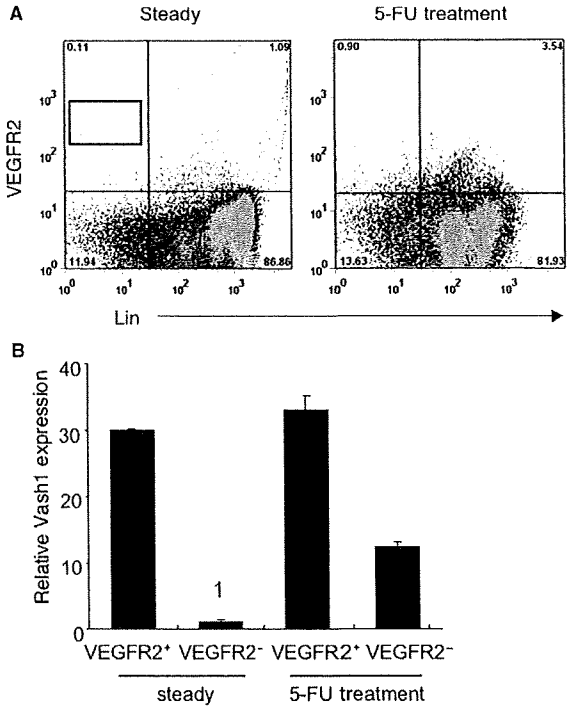

Fig. 3. **VEGFR2 expression by haematopoietic progenitors after treatment with 5-FU.** (A) BM cells from 10-week-old mice before and after (7 days) treatment with 5-FU were stained for lineage markers and antibody against VEGFR2. Note that $Lin^-VEGFR2^{high}$ cells indicated by the box disappeared after treatment with 5-FU. (B) qRT–PCR for *VASH1* in different cell populations from adult BM before and after treatment with 5-FU as shown in (A).

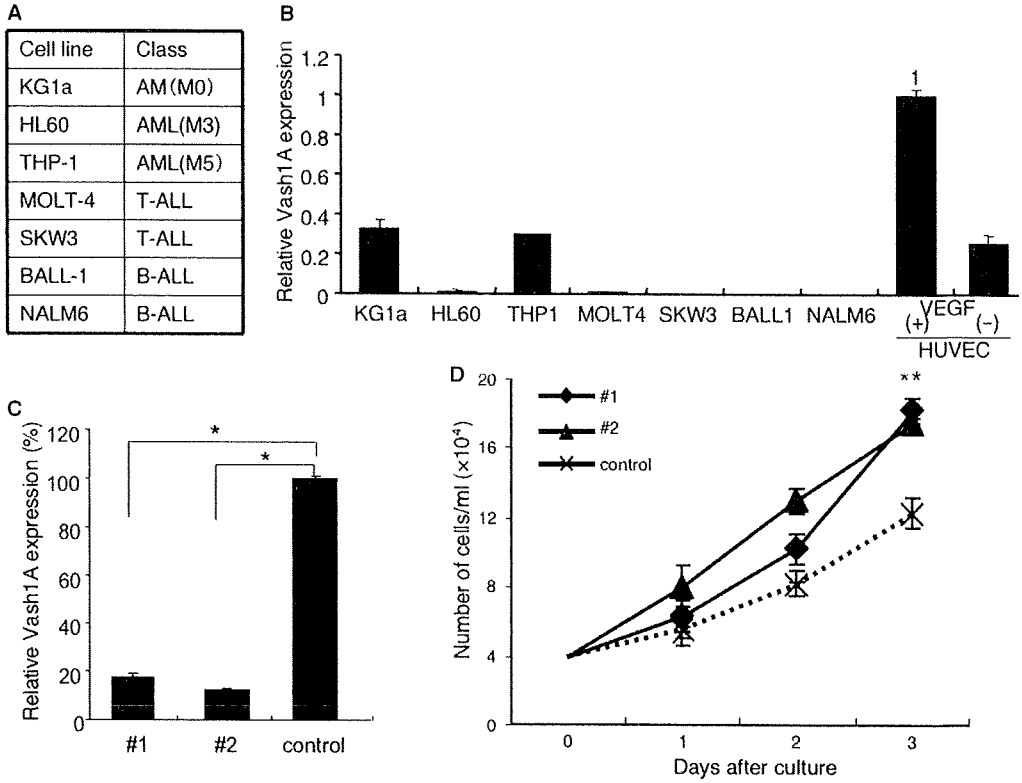

Fig. 4. **Expression of VASH1A in leukaemic cell lines.** (A) Leukaemic cell lines used in this experiment. (B) qRT–PCR for *VASH1A* in different leukaemic cells. HUVECs stimulated with (+) or without (−) VEGF were used as positive controls. (C) qRT-PCR for *VASH1A* after silencing by two RNAis (#1 and #2) or a control RNAi (control). $^{*}P<0.05$ ($n=3$, mean ± SD). (D) Cell growth after introduction of RNAi as described in (C). $^{**}P<0.05$ ($n=3$, mean ± SD).

HUVECs as a positive control and confirmed that VEGF induces *VASH1A* expression in HUVECs as previously reported (*12*) (Fig. 4B).

As it has been suggested the existence of alternatively splicing short forms of *VASH1A* termed *VASH1B*, we detected *VASH1B* in these two leukaemia cell line (KG1a and THP1) at a similar extent with *VASH1A* (data not shown).

Using RNAi methodology targeting two different cording regions of the human *Vash1* mRNA sequence, we then tested the effect of blocking VASH1 on cell growth. For reasons that remain unclear, this approach was not successful technically with KG1a cells, but *VASH1A* expression in THP1 cells could be greatly attenuated in this way (Fig. 4C). Proliferation of cells in which *VASH1A* had been knocked down was significantly greater than in controls, suggesting that attenuation of VASH1A expression enhances cell proliferation (Fig. 4D).

DISCUSSION

It has been reported that VASH1 expression is induced in ECs after stimulation with VEGF or bFGF and that this factor then inhibits their proliferation and migration. Therefore, it has been suggested that VASH1 acts as a negative feedback regulator for angiogenesis to inhibit overgrowth of blood vessels. In the BM, SP cells are suggested to be the most immature HSC population that can be serially transplantable into lethally irradiated mice. As most SP cells are dormant and most likely adhere to osteoblasts in the BM (*21*), it is possible that VASH1 inhibits SP cell-cycle progression in such BM niches. To address this, an HSC-specific conditional knock-out of the *VASH1* gene will be required. However, thus far molecules specifically expressed on SP cells have not been well documented, with the exception of ABCG2, an ABC transporter. Therefore, we propose that our present data identifying a novel molecule expressed on SP cells will be useful at least as a marker.

It is of note that VASH1 expression was induced in HPs, but not HSCs, during recovery from BM ablation. It had been considered that surviving HSCs in the BM start to self-renew and subsequently HPs derived from these HSCs acutely proliferate. However, in HSC division, it is not clear whether a single HSC gives rise to two HSC by symmetrical cell division or whether one HSC and one progenitor are produced by asymmetric cell division. Of course, it is possible that both types of cell division occur, but the mechanisms responsible for controlling when HSCs stop dividing remain obscure. If VASH1 has a role in maintaining HSC pool size in the BM by inhibiting cell growth, it would be expected that VASH1 expression should be induced in this population during recovery after BM ablation. However, VASH1 expression in HSCs was not affected by treatment

with 5-FU, suggesting that their cell division occurs very early after ablation of the BM and stops soon after giving rise to daughter progenitor cells.

During the recovery stage, HPs proliferate acutely; however, their cell division needs to be downregulated again after sufficient mature HCs have been generated. The mechanism responsible for this negative feedback regulation has thus far eluded identification. Our results presented here suggest that VASH1 might be a one of the negative regulators active at the final stage of acute recovery following BM ablation, because knockdown of the *VASH1A* gene-enhanced proliferation of VASH1A$^+$ cells from leukaemic lines.

Currently, it is thought that the expression of VASH1 and VEGFR2 is reciprocally cross-regulated in ECs (*17*). Attenuation of VEGFR2 expression by VASH1 may reduce responsiveness to VEGF, resulting in inhibition of angiogenesis. In the present study, HPs highly expressing VEGFR2 disappeared during recovery from BM ablation. It has been reported that VEGF promotes proliferation of HPs (*25*). Therefore, upregulation of VASH1 on HPs may reduce the expression of VEGFR2 as a means of negative feedback regulation of HP proliferation. Regulation of VEGFR2 expression by HPs may be part of the mechanism controlling the function of VASH1 in haematopoiesis. However, VEGFR2$^+$ HPs represent a very minor population among HPs. Therefore, other molecules must be involved in the negative regulation of cell growth in haematopoiesis. To understand the precise mechanism, targeted disruption of the VASH1 gene in HPs is required. This would enable the determination of the precise function of VASH1 in HP proliferation and negative feedback regulation to maintain HP pool size.

ACKNOWLEDGEMENT

We thank Mrs K. Fukuhara and N. Fujimoto for technical assistance.

FUNDING

This work was partly supported by the Japanese Ministry of Education, Culture, Sports, Science and Technology and the Japan Society for Promotion of Science.

CONFLICT OF INTEREST

None declared.

REFERENCES

1. Choi, K., Kennedy, M., Kazarov, A., Papadimitriou, J.C., and Keller, G. (1998) A common precursor for hematopoietic and endothelial cells. *Development* **125**, 725–732
2. Nishikawa, S.I., Nishikawa, S., Kawamoto, H., Yoshida, H., Kizumoto, M., Kataoka, H., and Katsura, Y. (1998) *In vitro* generation of lymphohematopoietic cells from endothelial cells purified from murine embryos. *Immunity* **8**, 761–769
3. Yamada, Y. and Takakura, N. (2006) Physiological pathway of differentiation of hematopoietic stem cell population into mural cells. *J. Exp. Med.* **203**, 1055–1065
4. Sata, M., Saiura, A., Kunisato, A., Tojo, A., Okada, S., Tokuhisa, T., Hirai, H., Makuuchi, M., Hirata, Y., and Nagai, R. (2002) Hematopoietic stem cells differentiate into vascular cells that participate in the pathogenesis of atherosclerosis. *Nat. Med.* **8**, 403–409
5. Sugiyama, T., Kohara, H., Noda, M., and Nagasawa, T. (2006) Maintenance of the hematopoietic stem cell pool by CXCL12-CXCR4 chemokine signaling in bone marrow stromal cell niches. *Immunity* **25**, 977–988
6. Avecilla, S.T., Hattori, K., Heissig, B., Tejada, R., Liao, F., Shido, K., Jin, D.K., Dias, S., Zhang, F., Hartman, T.E., Hackett, N.R., Crystal, R.G., Witte, L., Hicklin, D.J., Bohlen, P., Eaton, D., Lyden, D., de Sauvage, F., and Rafii, S. (2004) Chemokine-mediated interaction of hematopoietic progenitors with the bone marrow vascular niche is required for thrombopoiesis. *Nat. Med.* **10**, 64–71
7. Takakura, N., Watanabe, T., Suenobu, S., Yamada, Y., Noda, T., Ito, Y., Satake, M., and Suda, T. (2000) A role for hematopoietic stem cells in promoting angiogenesis. *Cell* **102**, 199–209
8. Takakura, N. (2006) Role of hematopoietic lineage cells as accessory components in blood vessel formation. *Cancer Sci.* **97**, 568–574
9. Coussens, L.M., Raymond, W.W., Bergers, G., Laig-Webster, M., Behrendtsen, O., Werb, Z., Caughey, G.H., and Hanahan, D. (1999) Inflammatory mast cells up-regulate angiogenesis during squamous epithelial carcinogenesis. *Genes Dev.* **13**, 1382–1397
10. Hiratsuka, S., Nakamura, K., Iwai, S., Murakami, M., Itoh, T., Kijima, H., Shipley, J.M., Senior, R.M., and Shibuya, M. (2002) MMP9 induction by vascular endothelial growth factor receptor-1 is involved in lung-specific metastasis. *Cancer Cell* **2**, 289–300
11. Ribatti, D., Presta, M., Vacca, A., Ria, R., Giuliani, R., Dell'Era, P., Nico, B., Roncali, L., and Dammacco, F. (1999) Human erythropoietin induces a pro-angiogenic phenotype in cultured endothelial cells and stimulates neovascularization in vivo. *Blood* **93**, 2627–2636
12. Watanabe, K., Hasegawa, Y., Yamashita, H., Shimizu, K., Ding, Y., Abe, M., Ohta, H., Imagawa, K., Hojo, K., Maki, H., Sonoda, H., and Sato, Y. (2004) Vasohibin as an endothelium-derived negative feedback regulator of angiogenesis. *J. Clin. Invest.* **114**, 898–907
13. Nimmagadda, S., Geetha-Loganathan, P., Pröls, F., Scaal, M., Christ, B., and Huang, R. (2007) Expression pattern of Vasohibin during chick development. *Dev. Dyn.* **236**, 1385–1362
14. Sonoda, H., Ohta, H., Watanabe, K., Yamashita, H., Kimura, H., and Sato, Y. (2006) Multiple processing forms and their biological activities of a novel angiogenesis inhibitor vasohibin. *Biochem. Biophys. Res. Commun.* **342**, 640–646
15. Kern, J., Bauer, M., Rychli, K., Wojta, J., Ritsch, A., Gastl, G., Gunsilius, E., and Untergasser, G. (2008) Alternative splicing of vasohibin-1 generates an inhibitor of endothelial cell proliferation, migration, and capillary tube formation. *Arterioscler. Thromb. Vasc. Biol.* **28**, 478–484
16. Shibuya, T., Watanabe, K., Yamashita, H., Shimizu, K., Miyashita, H., Abe, M., Moriya, T., Ohta, H., Sonoda, H., Shimosegawa, T., Tabayashi, K., and Sato, Y. (2006) Isolation and characterization of vasohibin-2 as a homologue of VEGF-inducible endothelium-derived angiogenesis inhibitor vasohibin. *Arterioscler. Thromb. Vasc. Biol.* **26**, 1051–1057
17. Shen, J., Yang, X., Xiao, W.H., Hackett, Y., Sato, Y., and Campochiaro, P.A. (2006) Vasohibin is up-regulated by VEGF in the retina and suppresses VEGF receptor 2 and retinal neovascularization. *FASEB J.* **20**, 723–725
18. Yamashita, H., Abe, M., Watanabe, K., Shimizu, K., Moriya, T., Sato, A., Satomi, S., Ohta, H., Sonoda, H., and Sato, Y. (2006) Vasohibin prevents arterial neointimal formation through angiogenesis inhibition. *Biochem. Biophys. Res. Commun.* **345**, 919–925

19. Yoshinaga, K., Ito, K., Moriya, T., Nagase, S., Takano, T., Niikura, H., Yaegashi, N., and Sato, Y. (2008) Expression of vasohibin as a novel endothelium-derived angiogenesis inhibitor in endometrial cancer. *Cancer Sci.* **99**, 914–919
20. Goodell, M.A., Brose, K., Paradis, G., Conner, A.S., and Mulligan, R.C. (1996) Isolation and functional properties of murine hematopoietic stem cells that are replicating *in vivo*. *J. Exp. Med.* **183**, 1797–1806
21. Arai, F., Hirao, A., Ohmura, M., Sato, H., Matsuoka, S., Takubo, K., Ito, K., Koh, G.Y., and Suda, T. (2004) Tie2/angiopoietin-1 signaling regulates hematopoietic stem cell quiescence in the bone marrow niche. *Cell* **118**, 149–161
22. Kidoya, H., Ueno, M., Yamada, Y., Mochizuki, N., Nakata, M., Yano, T., Fujii, R., and Takakura, N. (2008) Spatial and temporal role of the apelin/APJ system in the caliber size regulation of blood vessels during angiogenesis. *EMBO J.* **27**, 522–534
23. Kinnaird, T., Stabile, E., Burnett, M.S., and Epstein, S.E. (2004) Bone-marrow-derived cells for enhancing collateral development: mechanisms, animal data, and initial clinical experiences. *Circ. Res.* **95**, 354–363
24. Darnowski, J.W. and Handschumacher, R.E. (1985) Tissue-specific enhancement of uridine utilization and 5-fluorouracil therapy in mice by benzylacyclouridine. *Cancer Res.* **45**, 5364–5368
25. Smith, S.L., Agbemadzo, B., Reems, J.A., Tyler, T., Kiss, J., and Moldwin, R.L. (2000) Expansion of CD34+KDR+cells in cord blood after culture with TPO, FLT-3L, SCF, and VEGF. *Exp. Hematol.* **28**, 94
26. Rafii, S., Avecilla, S., Shmelkov, S., Shido, K., Tejada, R., Moore, M.A., Heissig, B., and Hattori, K. (2003) Angiogenic factors reconstitute hematopoiesis by recruiting stem cells from bone marrow microenvironment. *Ann. NY Acad. Sci.* **996**, 49–60

Biochemical and Biophysical Research Communications 380 (2009) 609–613

Contents lists available at ScienceDirect

Biochemical and Biophysical Research Communications

journal homepage: www.elsevier.com/locate/ybbrc

Identification and characterization of stem cell-specific transcription of *PSF1* in spermatogenesis

Yinglu Han, Masaya Ueno, Yumi Nagahama, Nobuyuki Takakura *

Department of Signal Transduction, Research Institute for Microbial Diseases, Osaka University, 3-1, Yamada-oka, Suita, Japan

ARTICLE INFO

Article history:
Received 22 January 2009
Available online 27 January 2009

Keywords:
DNA replication
Testis development
Promoter
PSF1
Stem cell

ABSTRACT

PSF1 is an evolutionarily conserved DNA replication factor, which forms the GINS complex with PSF2, PSF3, and SLD5. The mouse *PSF1* homolog has been identified from a stem cell-specific cDNA library. To investigate its transcriptional regulatory mechanisms during differentiation, we studied *PSF1* mRNA expression in testis and characterized its promoter. No canonical TATA or CAAT boxes could be found in the *PSF1* 5′-flanking region, whereas several consensus AML1, GATA, and Sry putative binding sequences are predicted within 5 kb of the putative transcription start site. In addition, binding sites for oncoproteins such as Myb and Ets were also found in the promoter. In testis, various *PSF1* gene transcription initiation sites are present and short transcripts encoding two novel isoforms, PSF1b and 1c, were found. However, spermatogonium stem cells specifically express transcripts for PSF1a. These data suggest that PSF1 is tightly regulated at the transcriptional level in stem cells.

Because of the finite life span of most mature cells, tissue stem cells, and progenitors are required to supply replacements by proliferation and differentiation. Particularly, testis and bone marrow (BM) stem cells continuously self-renew and also produce differentiated cell lineages. Hematopoietic stem cells (HSCs) and spermatogonial stem cells (SSCs) have a high regenerative capacity. In a mouse experimental model, one single HSC was found to be sufficient to reconstitute hematopoiesis when transplanted into a BM-ablated recipient [1]. When spermatogenesis is disrupted by high temperatures or drugs, surviving SSCs can regenerate spermatogenesis [2,3]. Because these tissue stem cells have great regenerative capacity for reconstituting ablated tissues, ex vivo amplification of stem cells without loss of self-renewal and multidifferentiation potential represents an important target for transplantation, gene, and cellular therapies. In order to study the molecular mechanisms regulating self-renewal of stem cells, knock-out (KO) mice lacking several cell cycle-related genes, such as p27, p18, and ATM, were generated as previously reported [4–6]. However, their downstream function in the self-renewal process, especially regarding molecules involved in DNA replication, is currently not known.

The initiation of DNA replication in eukaryotic cells is mediated by a highly ordered series of steps involving multiple complexes at replication origins [7,8]. This process commences with the binding of the origin recognition complex (ORC) to replication origins. CDC6 and Cdt1 bind to ORCs to act as loading factors for the Mcm2-7 (minichromosome maintenance) complex and then pre-replication complexes (pre-RC) are established. At the G1/S transition of the cell cycle, the pre-RCs are transformed into initiation complexes (ICs). Activation of MCM helicase activity requires the action of two protein kinases, DDK (Cdc7-Dbf4) and CDK (cyclin-dependent), as well as the participation of at least eight additional factors, including Mcm10, Cdc45, Dpb11, synthetic lethal with dpb11 mutant-2 (Sld2), Sld3, and GINS [9]. GINS was recently identified as a novel heterotetrameric complex from lower eukaryotes. It consists of four subunits, SLD5, PSF1, PSF2, and PSF3, each of approximately 200 amino acid residues highly conserved in all eukaryotes and essential for both the initiation and progression of DNA replication [10–12].

By using lower eukaryote models, multiple steps for progression of DNA replication are now well understood at the protein level, e.g. phosphorylation, degradation, and/or interaction processes; however, how these factors are activated or inactivated at the RNA level in mammalian tissues consisting of multiple cell lineages and cells in different phases of the cycle has not been elucidated. Previously, we cloned the mouse ortholog of *PSF1* and *SLD5* from an HSC-specific cDNA library or by two-hybrid screening of a cDNA library derived from embryos [13,14]. Transcription of *PSF1* is predominantly found in highly proliferative tissues, such as BM and testis. Loss of *PSF1* causes embryonic lethality around the implantation stage [13], with *PSF1*$^{-/-}$ embryos showing impaired proliferation of multipotent stem cells, i.e., the inner cell mass. However, the transcriptional regulation of *PSF1* in immature cells is not understood.

Abbreviations: GINS, Go-ichi-nii-san; PSF, partner of SLD5; SSCs, sperm stem cells; HSCs, hematopoietic stem cells

* Corresponding author. Fax: +81 6 6879 8314.
E-mail address: ntakaku@biken.osaka-u.ac.jp (N. Takakura).

0006-291X/$ - see front matter © 2009 Elsevier Inc. All rights reserved.
doi:10.1016/j.bbrc.2009.01.133

Here, we have isolated the 5′ promoter sequence of the *PSF1* gene to investigate regulatory mechanisms responsible for tissue-specific expression. We report an in silico analysis of the potential *cis*-regulatory elements in the *PSF1* promoter. In addition, we studied SSC-specific transcription initiation sites and multiple transcription initiation sites of *PSF1* in testis.

Materials and methods

Animals. ICR mice were purchased from Japan SLC (Shizuoka, Japan). All animal studies were approved by the Osaka University Animal Care and Use Committee.

In situ hybridization. cDNA fragments were amplified by PCR using the primer set 5′-GAA TTC AAA GCT TTG TAT GAA CAA AAC CAG-3′ and 5′-GTC GAC TCA GGA CAG CAC GTG CTC TAG AAC T-3′, followed by ligation into pT7 Blue Vector (Novagen Inc., Madison, WI, USA). These plasmids were used for probe synthesis. Antisense and sense cRNA probes were synthesized using digoxigenin (DIG)-RNA labeling kits with T7 RNA polymerase (Roche Diagnostics, Indianapolis, IN, USA). Hybridization was performed as previously described [15].

Cell culture. Colon 26 cells were maintained in DMEM medium containing 10% FBS, 100 IU penicillin and 100 μg/ml streptomycin. The cells were plated in 10 cm tissue culture dishes in 5% CO_2 and 95% air at 37 °C.

5′-Rapid amplification of cDNA ends (5′-RACE). 5′-RACE was performed as described previously [16]. In brief, we used the 5′ RACE System for Rapid Amplification of cDNA Ends (Invitrogen, Carlsbad, CA) according to the manufacturer's instructions. Total RNA was purified from whole testis, embryonic day (E) 10.5 embryos, colon 26 cells, and sorted cells (see below) by the guanidine-thiocyanate extraction method. Total RNA of sorted cells was purified using RNeasy Plus Mini Kits (Qiagen, Valencia, CA) according to manufacturer's instructions. *PSF1* transcripts were reverse-transcribed with Superscript II (Invitrogen) using the gene-specific primer PSF1GSP1 5′-GCA TGT CTG TCA ATT TAA-3′. The products were poly(C) tailed by terminal deoxynucleotidyl transferase and amplified by PCR, using an anchor primer and the gene-specific primer 5′-CGA AGC AAC CGG TCA TAC A-3′ (PSF1ANGSP1). The amplified products were subcloned into pT7 Blue vector (Novagen).

5′ End amplification of PSF1 cDNA using 5′ End oligo-capped cDNA library. CapSite cDNA (Nippon Gene., Toyama, Japan) from mouse testis and embryo (Day15) was used as a template for PCR with primer 1RC (Nippon gene., Toyama, Japan) corresponding to the oligoribonucleotide sequence ligated at the cap site and a *PSF1* gene-specific primer, 5′-CGA AGC AAC CGG TCA TAC A-3′ (PSF1ANGSP1) and the PCR product was then used as a template for the second round PCR with nested primers 2RC (Nippon Gene) and 5′-GCTATCGTGCAGCGTCTATT-3′ (PSF1ANGSP2). The amplified products were used for Southern blotting or purified, cloned and sequenced.

Southern blotting. Amplified 5′-ends of cDNA by 5′-RACE (see above) were separated on 0.8% agarose gels and transferred onto nylon membrane filters which were hybridized overnight at 60 °C in DIG Easy Hyb (Roche Diagnostics, Germany) with a digoxigenin-labeled *PSF1* cDNA probe. The hybridized probe was detected with alkaline phosphatase-conjugated antidigoxigenin antibodies using the DIG luminescent detection kit (Roche), following the manufacturer's instructions. The probe was prepared by using PCR DIG Probe Synthesis Kits (Roche) with primers: E11prb-2s (5′-AGC TGG TTG CTG GTG TTG TGC GAC-3′) and E11prb-2r (5′-CGA AAA CAA GAA ACG CTC AGA TGG G-3′).

Enrichment of SSCs. Isolation of SSCs was as previously reported [17]. Briefly, experimental cryptorchid testes were produced by suturing the testis fat pad to the abdominal wall at 7 weeks of age. After 2 or 3 months, testes were dissected and then digested with collagenase (Type IV, Sigma, St Louis, MO) at 32 °C for 15 min. The cells were next digested with DNase (Sigma) and trypsin (GIBCO) at 32 °C for 10 min. When most of the cells were dispersed, the action of trypsin was terminated by adding PBS containing 1% fetal bovine serum. Cell sorting was performed as described previously [18]. The antibody used for detection of SSCs was a FITC-conjugated anti-α6-integrin antibody (BD Biosciences. San Jose, CA). Control cells were stained with isotype-matched control antibodies. After the final wash, cells were resuspended in 2 ml of PBS/FBS containing 1 μg/ml propidium iodide for identification of dead cells. The stained cells were analyzed by FACS Calibur (Becton & Dickinson, New Jersey, USA), and sorted by JSAN (Bay Bioscience, Kobe, Japan).

Results and discussion

Proliferating germ cells express high levels of PSF1 transcripts

Previously we reported that *PSF1* transcripts are highly expressed in testis and BM [13]. In addition, immunohistochemistry also revealed the presence of PSF1 protein specifically in the spermatogonia, lining the outermost layer of the testis [13]. Here, to study the expression of *PSF1* mRNA in the testis, we performed in situ hybridization with an antisense-probe which hybridized to spermatogonia (arrow) and spermatocytes (arrowhead) (Fig. 1A). No obvious signals were recorded when using the sense-probe (Fig. 1B). These data indicate that stem cell-specific expression of PSF1 may be regulated at the transcriptional or post-transcriptional level, because although PSF1 protein could be detected in the spermatogonia this was not the case in spermatocytes [13].

Identification and characterization of PSF1 transcription initiation sites

In order to identify the *PSF1* promoter, we performed 5′-RACE analysis with *PSF1* gene-specific primers. Total RNA from testis, colon 26 cells, and whole embryo were reverse-transcribed (see Materials and methods). Although a single DNA band <372 bp in length was obtained after nested PCR of colon 26 and whole embryo, a broad band was amplified from testis cDNA (Fig. 1C,a). We also observed smaller transcripts in 5′ End amplificated cDNA of *PSF1* using 5′ End oligo-capped cDNA library from testis compared to that from embryo (Fig. 1C,b). To exclude that this was caused by degraded RNA in our sample, total RNA was visualized by Ethidum bromide (Fig. 1D). The quality of the RNA in each sample was essentially the same. Thus, the broad band seen in testis was not caused by RNA degradation. We then amplified each cDNA fragment, purified them and subcloned them for DNA sequencing. Here, the 5′-end of the longest cDNA fragment is defined as "+1" (Table 1, +1 5′-TGC ACT TCT ATT-3"). It was located 157 bp upstream of the first ATG.

Putative cis elements of the 5′-flanking regions of PSF1

To characterize the 5′-flanking region of PSF1, we analyzed putative transcription binding sites in silico (Fig. 3). The proximal 5′-flanking region of the *PSF1* gene lacks consensus CAAT or TATA boxes, but possesses consensus Sp1 binding sites, which are characteristic of TATA-less gene promoters [19]. In the 5′-flanking region of *PSF1*, several putative *cis*-acting elements were identified, such as E2F, GATA, Myb, AML1, Evi-1, and Sry.

As previously reported, E2F is known to regulate DNA replication, cell cycle progression, DNA repair, and differentiation

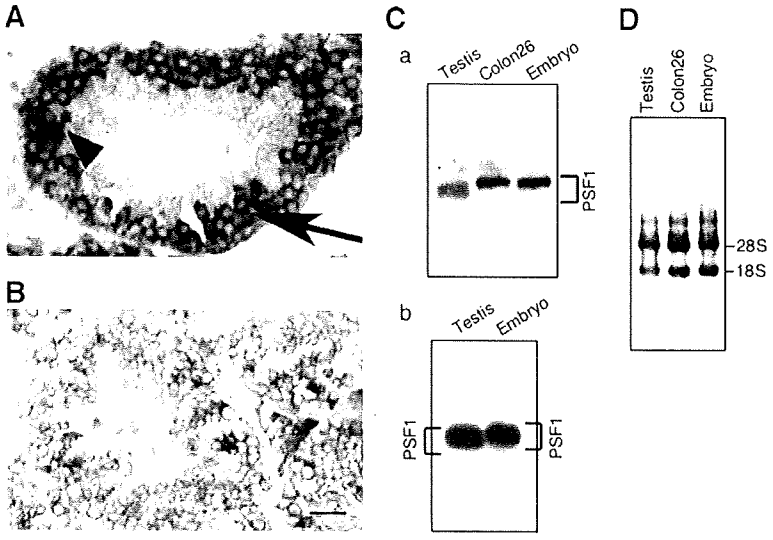

Fig. 1. *PSF1* expression in adult testis. (A) Antisense or (B) sense-probes for detection of *PSF1* were hybridized on sections of adult testis. Arrow, spermatogonia; arrowhead, spermatocyte. Bar indicates 20 μm. (C) Southern blot analysis of 5′-RACE product (a) and 5′ End amplificated cDNA of *PSF1* using 5′ End oligo-capped cDNA library (b) hybridized with a *PSF1* cDNA probe. Note that diffuse short bands are found in testis. (D) Ethidium bromide staining of total RNAs used in (C).

Table 1
Positions of 5′-RACE products of PSF1 transcripts.

Tissue or cells	Position of 5′-end	Translation		
		PSF1a	PSF1b	PSF1c
Colon 26	1, 20, 20, 20, 30, 30, 37, 42, 70, 70, 74, 227	92	0	8
Embryo	20, 30, 30, 30, 32, 35, 38, 47, 49, 50, 53, 57, 66, 72, 73, 117, 160	94	6	0
Testis	16, 22, 24, 25, 28, 28, 30, 30, 36, 66, 70, 70, 70, 70, 71, 73, 73, 73, 100, 107, 107, 113, 113, 113, 113, 113, 121, 130, 130, 146, 155, 155, 155, 161, 165, 165, 165, 165, 165, 165, 178, 178, 182, 182, 182, 182, 182, 186, 191, 193, 193, 193, 193, 213, 227, 230	59	13	28
SSCs	ND[a]	100[b]	0[b]	0[b]

[a] ND, No data.
[b] Percents are determined by PCR.

[20,21]. Moreover, E2F-1 is expressed in $CD34^+$ human hematopoietic stem and progenitor cells [22], and may play a critical role in hematopoiesis. Myb, AML1, and Evi-1 are also essential for HSC development [23–25]. GATA-1 does have a critical role in fate decision of HSCs [26]. Although GATA-2 has been suggested to play a role in maintenance of HSCs from the observation of GATA-$2^{-/-}$ mice [27], it remains indeterminate whether GATA-2 enhances or suppresses the growth of HSCs [28–31]. As high level expression of PSF1 is observed in hematopoietic organs and testis in the adulthood, suggesting that these transcription factors may contribute to stem cell-specific transcription in testis as well as hematopoietic organs.

Multiple translation initiation sites

In our 5′-RACE analysis, small cDNA fragments were found specifically in testis (Fig. 2 and Table 1). Therefore, we next analyzed the translation initiation sites of each cDNA fragment (Fig. 3 and Table 1). ATG was present first in most of the transcripts tested in colon 26 and whole embryo, suggesting that these are translated to full-length PSF1 (PSF1a). However, in testis, there were many short transcripts which may be translated to truncated forms of PSF1 (PSF1b or PSF1c). Putative PSF1b lacks 6 amino acid residues and putative PSF1c lacks a partial portion of a coiled-coil domain compared to the PSF1 protein. The DNA sequences from the RT-PCR products of 5′ End amplifications using 5′ End oligo-capped cDNA library showed that 1.2% of the transcripts derived from testis were PSF1a type and the remnants were PSF1b and PSF1c. On the other hand, transcripts derived from embryo were almost exclusively PSF1a type. These data suggest that the short PSF1 transcripts may be translated into the truncated forms PSF1b and PSF1c specifically in testis.

SSCs express only the PSF1a isotype

Next, to investigate which RNAs are transcribed in sperm stem cells (SSCs, spermatogonia), we sorted these cells (Fig. 4A) and performed 5′-RACE analysis (Fig. 4B and Table 1). In contrast to whole testis, only one band was amplified from SSCs. After purification, we assessed the cDNA using PCR and found that amplificates contained ATG first, suggesting that only PSF1a is expressed in SSCs (Table 1).

We detected PSF1 protein in spermatogonia but not in spermatocytes by immunohistochemical analysis [13], although in situ hybridization revealed that primary and secondary spermatocytes as well as spermatogonia contained PSF1 transcripts. We found that SSCs express PSF1a but not PSF1b or PSF1c. These results suggest that the PSF1b and 1c RNA which is present in primary and secondary spermatocytes may be unstable and degrade easily.

In summary, we identified several *PSF1* transcription initiation sites. Various small cDNA fragments of *PSF1* were derived from testis, suggesting that *PSF1* RNAs are translated into three isotypes. These alternative forms may generate functionally different PSF1 proteins, contributing to differences in the mechanism of prolifer-

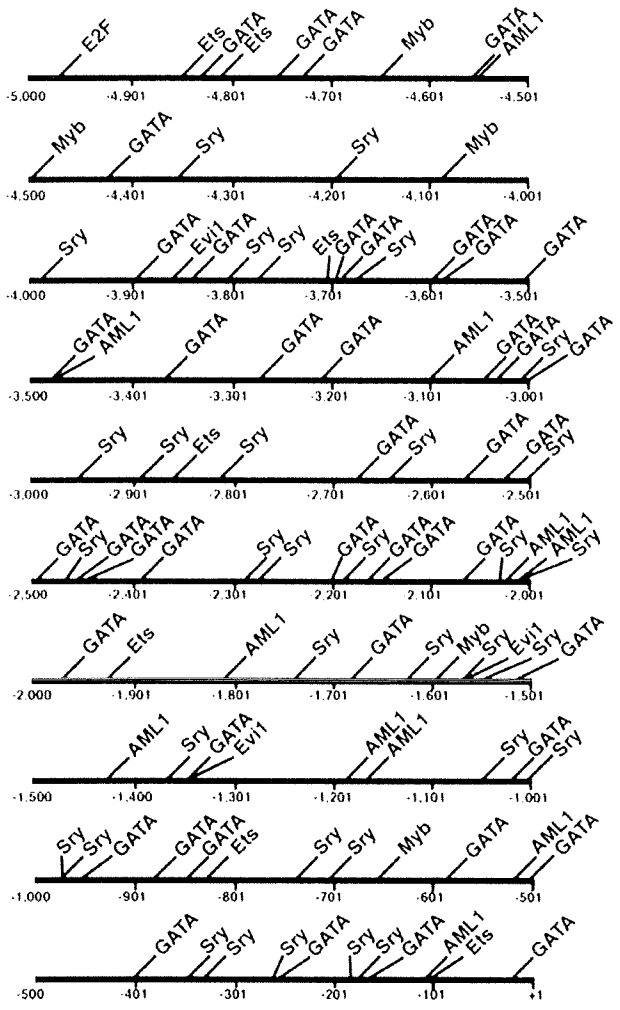

Fig. 2. Schematic representation of the putative transcriptional regulatory elements in the 5′-flanking region of the mouse *PSF1* gene. Consensus sequences of *cis*-regulatory elements in the *PSF1* promoter were sought in the TFSEARCH database (http://mbs.cbrc.jp/research/db/TFSEARCH.html). The numbers in parentheses indicate the positions of the first and last nucleotides of the elements.

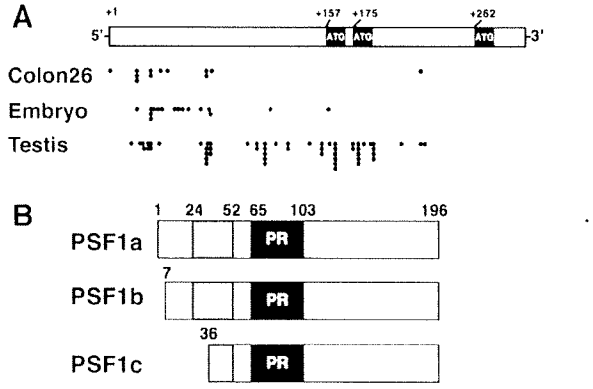

Fig. 3. Transcription initiation sites of *PSF1* and PSF1 isoforms. (A) Schematic representation of the summed data on transcription initiation sites. Each closed dot indicates the position of 5′-ends of 5′-RACE products. (B) Putative primary structures of PSF1 isoforms. Cc, N terminal region containing coiled-coil domain; PR, central region containing arginine-rich domain.

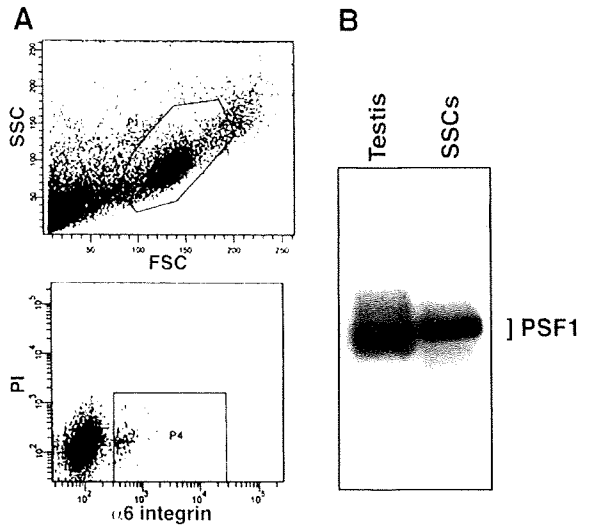

Fig. 4. Expression of *PSF1* gene in SSCs. (A) Flow cytometric analysis for sorting SSCs. Gated region for SSCs in SSC/FSC (upper) and α6-integrin$^+$ PI cells population (lower) is shown. (B) Southern blot analysis of 5′-RACE products hybridized with a *PSF1* cDNA probe. Diffuse short bands were found in whole testis (Testis). SSCs, spermatogonium stem cells.

ation control in stem cells and progenitor cells. Further analysis of the regulatory mechanisms influencing PSF1 expression are needed to shed more light on the complex mechanisms of "stemness" in mammalian cells.

Acknowledgments

We thank N. Fujimoto, Y. Shimizu, K. Ishida, M. Sato, and Y. Nakano for technical assistance. We also thank K. Fukuhara for secretarial assistance. This work was partly supported by the Japanese Ministry of Education, Culture, Sports, Science and Technology, and the Japan Society for Promotion of Science.

References

[1] M. Osawa, K. Hanada, H. Hamada, H. Nakauchi, Long-term lymphohematopoietic reconstitution by a single CD34-low/negative hematopoietic stem cell, Science 273 (1996) 242–245.
[2] Y. Nishimune, S. Aizawa, T. Komatsu, Testicular germ cell differentiation in vivo, Fertil. Steril. 29 (1978) 95–102.
[3] C.J. van Keulen, D.G. de Rooij, Spermatogonial stem cell renewal in the mouse. II. After cell loss, Cell Tissue Kinet. 6 (1973) 337–345.
[4] T. Cheng, Rodrigues N.S. Stier, D.T.. Scadden, Stem cell repopulation efficiency but not pool size is governed by p27 (kip1), Nat. Med. 6 (2000) 1235–1240.
[5] Y. Yuan, H. Shen, D.S. Franklin, D.T. Scadden, T. Cheng, In vivo self-renewing divisions of haematopoietic stem cells are increased in the absence of the early G1-phase inhibitor, p18INK4C, Nat. Cell Biol. 6 (2004) 436–442.
[6] K. Ito, A. Hirao, F. Arai, S. Matsuoka, K. Takubo, I. Hamaguchi, K. Nomiyama, K. Hosokawa, K. Sakurada, N. Nakagata, Y. Ikeda, T.W. Mak, T. Suda, Regulation of oxidative stress by ATM is required for self-renewal of haematopoietic stem cells, Nature 431 (2004) 997–1002.
[7] J.J. Blow, A. Dutta, Preventing re-replication of chromosomal DNA, Nat. Rev. Mol. Cell Biol. 6 (2005) 476–486.
[8] T.S. Takahashi, D.B. Wigley, J.C. Walter, Pumps, paradoxes and ploughshares: mechanism of the MCM2–7 DNA helicase, Trends Biochem. Sci. 30 (2005) 437–444.
[9] K. Labib, A. Gambus, A key role for the GINS complex at DNA replication forks, Trends Cell Biol. 17 (2007) 271–278.
[10] M. Kanemaki, A. Sanchez-Diaz, A. Gambus, K. Labib, Functional proteomic identification of DNA replication proteins by induced proteolysis in vivo, Nature 423 (2003) 720–724.
[11] Y. Kubota, Y. Takase, Y. Komori, Y. Hashimoto, T. Arata, Y. Kamimura, H. Araki, H. Takisawa, A novel ring-like complex of Xenopus proteins essential for the initiation of DNA replication, Genes Dev. 17 (2003) 1141–1152.
[12] Y. Takayama, Y. Kamimura, M. Okawa, S. Muramatsu, A. Sugino, H. Araki, H. Takisawa, GINS, a novel multiprotein complex required for chromosomal DNA replication in budding yeast, Genes Dev. 17 (2003) 1153–1165.

[13] M. Ueno, M. Itoh, L. Kong, K. Sugihara, M. Asano, N. Takakura, PSF1 is essential for early embryogenesis in mice, Mol. Cell. Biol. 25 (2005) 10528–10532.
[14] L. Kong, M. Ueno, M. Itoh, K. Yoshioka, N. Takakura, Identification and characterization of mouse PSF1-binding protein, SLD5, Biochem. Biophys. Res. Commun. 339 (2006) 1204–1207.
[15] N. Kimura, M. Ueno, K. Nakashima, T. Taga, A brain region-specific gene product Lhx6.1 interacts with Ldb1 through tandem LIM-domains, J. Biochem. 126 (1999) 180–187.
[16] M. Ueno, N. Kimura, K. Nakashima, F. Saito-Ohara, J. Inazawa, T. Taga, Genomic organization, sequence and chromosomal localization of the mouse Tbr2 gene and a comparative study with Tbr1, Gene 254 (2000) 29–35.
[17] T. Shinohara, K.E. Orwig, M.R. Avarbock, R.L. Brinster, Spermatogonial stem cell enrichment by multiparameter selection of mouse testis cells, Proc. Natl. Acad. Sci. USA 97 (2000) 8346–8351.
[18] N. Takakura, T. Watanabe, S. Suenobu, Y. Yamada, T. Noda, Y. Ito, M. Satake, T. Suda, A role for hematopoietic stem cells in promoting angiogenesis, Cell 102 (2000) 199–209.
[19] S.T. Smale, Transcription initiation from TATA-less promoters within eukaryotic protein-coding genes, Biochim. Biophys. Acta 1351 (1997) 73–88.
[20] N. Dyson, The regulation of E2F by pRB-family proteins, Genes Dev. 12 (1998) 2245–2262.
[21] B.D. Rowland, R. Bernards, Re-evaluating cell-cycle regulation by E2Fs, Cell 127 (2006) 871–874.
[22] U. Steidl, R. Kronenwett, U.P. Rohr, R. Fenk, S. Kliszewski, C. Maercker, P. Neubert, M. Aivado, J. Koch, O. Modlich, H. Bojar, N. Gattermann, R. Haas, Gene expression profiling identifies significant differences between the molecular phenotypes of bone marrow-derived and circulating human CD34+ hematopoietic stem cells, Blood 99 (2002) 2037–2044.
[23] M.L. Mucenski, K. McLain, A.B. Kier, S.H. Swerdlow, C.M. Schreiner, T.A. Miller, D.W. Pietryga, W.J. Scott Jr., S.S. Potter, A functional c-myb gene is required for normal murine fetal hepatic hematopoiesis, Cell 65 (1991) 677–689.
[24] T. Okuda, J. van Deursen, S.W. Hiebert, G. Grosveld, J.R. Downing, AML1, the target of multiple chromosomal translocations in human leukemia, is essential for normal fetal liver hematopoiesis, Cell 84 (1996) 321–330.
[25] P.R. Hoyt, C. Bartholomew, A.J. Davis, K. Yutzey, L.W. Gamer, S.S. Potter, J.N. Ihle, M.L. Mucenski, The Evi1 proto-oncogene is required at midgestation for neural, heart, and paraxial mesenchyme development, Mech. Dev. 65 (1997) 55–70.
[26] H. Iwasaki, K. Akashi, Myeloid lineage commitment from the hematopoietic stem cell, Immunity 26 (2007) 726–740.
[27] F.Y. Tsai, G. Keller, F.C. Kuo, M. Weiss, J. Chen, M. Rosenblatt, F.W. Alt, S.H. Orkin, An early haematopoietic defect in mice lacking the transcription factor GATA-2, Nature 371 (1994) 221–226.
[28] C. Heyworth, K. Gale, M. Dexter, G. May, T. Enver, A GATA-2/estrogen receptor chimera functions as a ligand-dependent negative regulator of self-renewal, Genes Dev. 13 (1999) 1847–1860.
[29] S. Ezoe, I. Matsumura, S. Nakata, K. Gale, K. Ishihara, N. Minegishi, T. Machii, T. Kitamura, M. Yamamoto, T. Enver, Y. Kanakura, GATA-2/estrogen receptor chimera regulates cytokine-dependent growth of hematopoietic cells through accumulation of p21(WAF1) and p27(Kip1) proteins, Blood 100 (2002) 3512–3520.
[30] K. Kitajima, M. Masuhara, T. Era, T. Enver, T. Nakano, GATA-2 and GATA-2/ER display opposing activities in the development and differentiation of blood progenitors, EMBO J. 21 (2002) 3060–3069.
[31] D.A. Persons, J.A. Allay, E.R. Allay, R.A. Ashmun, D. Orlic, S.M. Jane, J.M. Cunningham, A.W. Nienhuis, Enforced expression of the GATA-2 transcription factor blocks normal hematopoiesis, Blood 93 (1999) 488–499.

Both alleles of *PSF1* are required for maintenance of pool size of immature hematopoietic cells and acute bone marrow regeneration

Masaya Ueno,[1] Machiko Itoh,[2] Kazushi Sugihara,[3] Masahide Asano,[3] and Nobuyuki Takakura[1,2]

[1]Department of Signal Transduction, Research Institute for Microbial Diseases, Osaka University, Osaka; [2]Department of Stem Cell Biology, Cancer Research Institute, Kanazawa University, Kanazawa; and [3]Institute for Experimental Animals, Kanazawa University Advanced Science Research Center, Kanazawa, Japan

Hematopoietic stem cells (HSCs) have a very low rate of cell division in the steady state; however, under conditions of hematopoietic stress, these cells can begin to proliferate at high rates, differentiate into mature hematopoietic cells, and rapidly reconstitute ablated bone marrow (BM). Previously, we isolated a novel evolutionarily conserved DNA replication factor, *PSF1* (*partner of SLD5-1*), from an HSC-specific cDNA library. In the steady state, PSF1 is expressed predominantly in CD34$^+$KSL (c-kit$^+$/Sca-1$^+$/Lineage$^-$) cells and progenitors, whereas high levels of PSF1 expression are induced in KSL cells after BM ablation. In 1-year-old *PSF1*$^{+/-}$ mice, the pool size of stem cells and progenitors is decreased. Whereas young *PSF1*$^{+/-}$ mutant mice develop normally, are fertile, and have no obvious differences in hematopoiesis in the steady state compared with wild-type mice, intravenous injection of 5-fluorouracil (5-FU) is lethal in *PSF1*$^{+/-}$ mice, resulting from a delay in induction of HSC proliferation during ablated BM reconstitution. Overexpression studies revealed that PSF1 regulates molecular stability of other GINS components, including SLD5, PSF2, and PSF3. Our data indicate that PSF1 is required for acute proliferation of HSCs in the BM of mice. (Blood. 2009;113:555-562)

Introduction

Tissue regeneration is one of the most tightly controlled processes requiring an ordered program involving induction of proliferation and differentiation of damaged-tissue stem cells. In the normal state, hematopoietic stem cells (HSCs) undergo cell division at a very low rate. However, if the bone marrow (BM) is ablated by an anticancer drug or radioactivity, HSCs that are in a quiescent state are stimulated to proliferate and restore the BM; self-renewal of HSCs is involved in this process.[1] In a mouse experimental model, only one HSC was found to be sufficient to reconstitute the entire hematopoiesis.[2] In this system, it has been suggested that daughter cells derived from HSCs can either commit to a program of differentiation that will eventually result in production of mature, nonproliferating cells or retain HSC properties.

Several proteins thought to be involved in HSCs for induction of self-renewal, including Wnt and Notch ligand families, have been isolated[3-5]; however, what lies downstream of them in the signaling pathway, especially molecules involved in DNA replication, is not known.

PSF1 (partner of SLD5-1) is evolutionarily conserved and is involved in DNA replication in lower eukaryotes,[6-8] and human.[9] PSF1 forms a tetrameric complex (GINS complex) with SLD5, PSF2, and PSF3. Recently, crystal structure of the human GINS complex was reported.[10-13] In yeast, GINS complex associates with MCM2-7 complex and CDC45, and this C-M-G complex (CDC45-MCM2-7-GINS) regulates both the initiation and progression of DNA replication.[14-17]

Previously, we cloned the mouse ortholog of *PSF1* from an HSC-specific cDNA library.[18] *PSF1* is predominantly expressed in highly proliferative tissues, such as testis and BM. Loss of *PSF1* causes embryonic lethality around the implantation stage.[18] *PSF1*$^{-/-}$ embryos revealed impaired proliferation of multipotent stem cells, ie, the inner cell mass. In mice, *PSF1* is highly expressed in proliferating HSCs and the hematopoietic progenitor cells (HPCs). However, the biologic function of PSF1 in hematopoiesis is not understood.

In this study, we used *PSF1*$^{+/-}$ mice for studying the function of PSF1 in hematopoiesis. Here we show that haploinsufficiency of *PSF1* causes loss of regeneration capacity resulting from a delay in induction of acute proliferation of HSCs after BM ablation. Our data suggest that both alleles of *PSF1* are essential for acute proliferation of HSCs after BM ablation.

Methods

Mice

C57BL/6 mice were purchased from SLC (Shizuoka, Japan). *PSF1* mutant mice and *Runx1*-deficient mice (*Runx1*-deficient mice were a gift from Dr T. Watanabe, Tohoku University, Sendai, Japan) were maintained and bred as described.[18,19] All animal studies were approved by the Animal Care Committee of Kanazawa University and the Osaka University Animal Care and Use Committee. For BM ablation studies, 8-week-old wild-type and *PSF1*$^{+/-}$ mice were treated with a single tail vein injection of 5-fluorouracil (5-FU; 150 mg/kg body weight; Kyowa Hakko Kogyo, Tokyo, Japan).

Immunohistochemistry and FACS analysis

Tissue fixation, preparation of tissue sections, and staining of sections with antibodies were performed as described previously.[18] For immunohistochemistry of fetal liver (FL), rabbit anti-PSF1 antibody was used.[18] Horseradish

Submitted January 29, 2008; accepted September 7, 2008. Prepublished online as *Blood* First Edition paper, November 4, 2008; DOI 10.1182/blood-2008-01-136879.

The online version of this article contains a data supplement.

The publication costs of this article were defrayed in part by page charge payment. Therefore, and solely to indicate this fact, this article is hereby marked "advertisement" in accordance with 18 USC section 1734.

peroxidase-conjugated secondary antibodies were obtained from Jackson ImmunoResearch Laboratories (West Grove, PA). For immunocytochemistry, we used monoclonal anti-PSF1 antibody (Aho57.2; see next paragraph below) as a first antibody and Alexa 488–conjugated antirat IgG (Invitrogen, Carlsbad, CA) as a second antibody. Stained cells and the sections were observed using an Olympus IX-70 microscope equipped with UPlanFI 4/0.13 and LCPlanFI 20 /0.04 dry objective lenses (Olympus, Tokyo, Japan). Images were acquired with a CoolSnap digital camera (Roper Scientific, Trenton, NJ), and processed with Adobe Photoshop version 8.0.1 software (Adobe Systems, San Jose, CA).

For the generation of monoclonal anti-PSF1 antibodies, cDNA encoding the full-length protein sequence of PSF1 was amplified by polymerase chain reaction (PCR), and then cDNA was ligated into pGEX-4T-1 vector (GE Healthcare, Little Chalfont, United Kingdom) for the preparation of glutathione S-transferase (GST)–fusion proteins. PSF1-coding region was amplified from the mouse NIH3T3 cDNA using the primers 5′-GGA ATT CAT GTT CTG CGA AAA AGC TAT G-3′ (sense) and 5′-GGA ATT CTC AGG ACA GCA CGT GCT CTA GA-3′ (antisense) and was subsequently subcloned as a *Eco*RI-*Eco*RI fragment into the pGEX-4T-1 vector (GE Healthcare) in the correct reading frame to express the GST-PSF1 fusion protein. This construct was transformed into *Escherichia coli* JM109 strains (Toyobo Engineering, Osaka, Japan) to obtain GST-tagged fusion proteins. Recombinant GST-PSF1 was purified using glutathione-Sepharose 4B column (GE Healthcare) according to the manufacturer's instructions. Purified GST-fused proteins were used as antigen for immunization of rats, and rat/mouse hybridomas were established by standard procedures.[20] A stable hybridoma cell line, aho57.2, was obtained. The specificities of all antibodies were determined by immunoblotting and immunocytochemistry.

Preparation of FL and BM cells and fluorescence-activated cell sorter (FACS) analysis was as described previously.[21,22] The antibodies used in flow cytometric analysis for lineage marker (Lin) were fluorescein isothiocyanate– or phycoerythrin-conjugated Gr-1 (RB6-8C5), Mac-1 (M1/70), B220 (RA3-6B2), TER119, anti-CD4 (GK1.5), and anti-CD8 (53-6.72). Allophycocyanin-conjugated anti–c-kit (ACK2), and biotin-conjugated anti–Sca-1 and CD34 were also applied. Biotinylated anti–Sca-1 or CD34 was visualized with peridinin chlorophyll protein–streptavidin. These antibodies were purchased from BD Biosciences (San Jose, CA). The stained cells were analyzed by FACSCalibur (BD Biosciences) and sorted by JSAN (Bay Bioscience, Kobe, Japan). For immunocytochemistry of HSCs from 5-FU–treated BM, 300 $CD34^+$ KSL cells were isolated by sorting from BM obtained from 5 mice 4 days after 5-FU treatment. The average number of total BM mononuclear cells and $CD34^+$ KSL obtained from right and left femurs and tibias after treatment with 5-FU was 9.3 plus or minus 5.3×10^6 and 60 plus or minus 38, respectively.

For the analysis of apoptosis, cells were stained with anti–annexin V antibodies (eBioscience, San Diego, CA). For platelet analysis, blood from wild-type and mutant mice was obtained from the tail vein and collected in phosphate-buffered saline (PBS) containing 3.8 mM citric acid, 7.5 mM trisodium citrate, and 10 mM of dextrose (PBS–acid-citrate-dextrose). Cells were stained with fluorescein isothiocyanate–conjugated anti-CD41 antibody (eBioscience).

qRT-PCR

Total RNA was isolated using the RNAeasy Kit (QIAGEN, Valencia, CA) according to the manufacturer's instructions. RNA was reverse transcribed using the ExScript RT Reagent Kit (Takara, Kyoto, Japan). Quantitative reverse-transcription polymerase chain reaction (qRT-PCR) was performed using Platinum SYBR Green qPCR SuperMix-UDG (Invitrogen) on an Mx3000 system (Stratagene, La Jolla, CA). Levels of the specific amplified cDNAs were normalized to the level of glyceraldehydes-3-phosphate dehydrogenase (*GAPDH*) housekeeping control cDNA. We used the following primer sets: 5′-GAA GGG CTC ATG ACC ACA GT-3′ and 5′-GGA TGC AGG GAT GAT GTT CT-3′, for *GAPDH*, and 5′-CCG GTT GCT TCG GAT TAG AG-3′ and 5′-CTC CCA GCG ACC TCA TGT AA-3′ for *PSF1*.

Cell culture

The colony formation unit in culture (CFU-c) assay was performed as described previously.[21] A total of 2×10^2 KSL-Mac-$1^{-/lo}$ cells that had been sorted from the BM of wild-type or $PSF1^{+/-}$ mice were placed in 1 mL semisolid medium (MethoCult; StemCell Technologies, Vancouver, BC). After 10 days of culture, the number of colonies was counted.

For the analysis of sensitivity of HSCs to 5-FU, 10^3 KSL cells derived from wild-type or $PSF1^{+/-}$ mice were seeded onto semisolid medium and continuously cultured for 10 days with or without 5-FU (1 ng/mL to 1 μg/mL). Each condition was represented by at least 3 wells, and each experiment was performed in triplicate. To examine the number of apoptotic cells in the population of colony-forming cells, colonies grown in methylcellulose semisolid medium were harvested 6 days after the CFU-c assay was initiated, and the cells were stained with Cy5-conjugated anti–annexin V antibody (eBioscience).

Cell-cycle analysis

Cells were sorted by FACS and fixed in 70% ethanol overnight. After treatment with RNase A (0.5 mg/mL; Sigma-Aldrich, St Louis, MO), cells were labeled with 5 μg/mL propidium iodide (PI) and analyzed by FACSCalibur.

Transfection and immunoblot analysis

NIH3T3 cells were transfected with pEF-BOSE, pEF-flag-PSF1, pEF-Myc-SLD5, pEF-HA-PSF2, and/or pEF-VSVG-PSF3, and immunoblotting was performed as previously described.[23] GAPDH was detected with anti-GAPDH antibodies (Chemicon International, Temecula, CA) for endogenous protein control. Transfection efficiency of each plasmid was determined by qRT-PCR (see "qRT-PCR"). We used the following primer sets: 5′-ATG GAC TAC AAG GAC GAC GAT GAC-3′ and 5′-CTC CCA GCG ACC TCA TGT AA-3′ (for *FLAG-PSF1*); 5′-GAG ATG AAC CGA CTT GGA AAG GG-3′ and 5′-TCC TCA TCA CGC ATC TGT TC-3′ (for *VSVG-PSF2*); 5′-TAC GAT GTT CCA GAT TAC GCG GG-3′ and 5′-CAG GAT GTC GTC CAA AGA CA-3′ (for *HA-PSF3*); 5′-CTC ATC TCA GAA GAG GAT CTG GG-3′ and 5′-GTG TGG TCC ATA TAC TCT TTG-3′ (for *Myc-SLD5*).

Transplantation study

For the analysis of sensitivity of HSCs to 5-FU in vivo, 8-week-old mice were treated with 5-FU (see "Cell culture"), and after 1 day of 5-FU treatment, $PSF1^{+/+}$ or $PSF1^{+/-}$ BM mononuclear cells (Ly5.2, 4×10^5) were transplanted into lethally irradiated (8.5 Gy) recipients (Ly5.1) together with untreated normal Ly5.1 BM cells (2×10^5). Four weeks after transplantation, donor contribution was determined by FACS using anti-Ly5.1 (eBioscience) and anti-Lin antibodies mixture.

Results

PSF1 is predominantly expressed in proliferating immature hematopoietic cells

Previously, we reported that *PSF1* expression was predominantly observed in immature cell populations in embryonic and adult tissues, such as blastocysts and spermatogonium in the adult.[18] Moreover, *PSF1* expression was observed in immature hematopoietic cells (HCs) designated as Lin^- $c\text{-}kit^+$ $Sca\text{-}1^+$ (KSL) at the RNA expression level. To confirm whether PSF1 protein is expressed in HSCs or not, $CD34^-$ or $CD34^+$ KSL, $Lin^-c\text{-}kit^+Sca\text{-}1^-$ (KL) or Lin^+ cells from adult BM were sorted, and expression of PSF1 was determined in each fraction (Figure 1A). It has been reported that $CD34^-$ KSL cells in the adult mouse BM are dormant and represent HSCs with long-term marrow repopulating ability, whereas $CD34^+$ KSL cells are progenitors with short-term

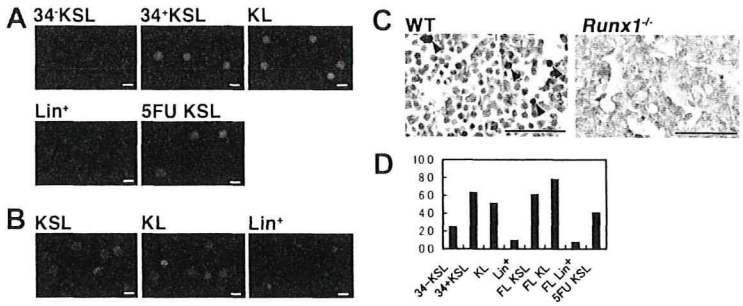

Figure 1. PSF1 expression in proliferating HSC population. (A,B) Immunostaining of several BM (A) or FL-derived (B) HC population with anti-PSF1 antibody. (A) CD34$^-$KSL (CD34$^-$c-kit$^+$Sca-1$^+$Lin$^-$ cells), 34$^+$KSL (CD34$^+$c-kit$^+$Sca-1$^+$Lin$^-$ cells), KL (c-kit$^+$Sca-1$^-$Lin$^-$ cells), Lin$^+$ (Lin$^+$ cells), and 5-FU KSL (5-FU-treated mouse derived CD34$^+$KSL cells). (B) KSL (c-kit$^+$Sca-1$^+$Lin$^-$ cells), KL (c-kit$^+$Sca-1$^-$Lin$^-$ cells), and Lin$^+$ (Lin$^+$ cells). Green color shows PSF1 staining. Nuclei were counterstained with PI (red). Bar represents 10 μm. (C) Sections of E12.5 FL from wild-type (WT) or *Runx1*$^{-/-}$ mice were stained with anti-PSF1 polyclonal antibody. Sections were counterstained with hematoxylin (original magnification ×400). Arrows indicate PSF1$^+$ cells. Bars represent 50 μm. (D) *PSF1* mRNA expression in various HC fractions of BM or FL cells as indicated in panel A. 5-FU KSL indicates KSL cells were sorted from BM of mice 4 days after treatment with 5-FU. The values were normalized to the amount of mRNA in Lin$^+$ cells from BM.

reconstitution capacity.[2,24] In the steady state, a high level of PSF1 expression was observed in CD34$^+$ KSL cells and KL cells, whereas a very low level of PSF1 expression was observed in CD34$^-$ KSL cells. However, no PSF1 expression was detected in mature cells (Lin$^+$; Figure 1A). It was reported that, after BM ablation, all HSCs express CD34 in a situation when BM is acutely reconstituted.[25] Therefore, to know whether PSF1 expression in HSCs correlates with cell cycle of HSCs, CD34$^+$ KSL cells were sorted from the BM 4 days after ablation of the BM by 5-FU. As expected, almost all CD34$^+$ KSL cells were stained by anti-PSF1 antibody (Figure 1A).

It is known that HSCs in the FL contain cells that cycle at a higher rate than those in the adult BM and HSCs express the Mac-1 antigen.[26] We sorted KSL (without Mac-1), KL, and Lin$^+$ cells from the FL at embryonic day (E) 12.5 and determined PSF1 expression. High PSF1 expression was found in both KSL and KL cells (Figure 1B), and Lin$^+$ cells did not express PSF1 as seen in the adult BM.

On immunohistochemistry, PSF1 expression was seen in a small population of round HCs in the FL at E12.5 (Figure 1C). However, in the adult liver, which is no longer a hematopoietic organ, PSF1 expression was not observed (data not shown). Furthermore, to test the specificity of this staining in the FL, we studied PSF1 expression in *Runx1*-deficient mice, which lack definitive hematopoiesis[27] and could not detect PSF1-positive cells in the FL in this mutant embryo (Figure 1C). To confirm the specific expression of PSF1 in proliferative and immature HCs, we performed qRT-PCR (Figure 1D). PSF1 was highly expressed in BM-derived CD34$^+$ KSL and Lin$^-$Kit$^+$, and FL-derived Lin$^-$Kit$^+$Sca1$^+$ and Lin$^-$Kit$^+$ cells. KSL cells derived from BM at 4 day after 5-FU treatment also expressed higher amounts of *PSF1* transcript than CD34$^-$ KSL cells. These results demonstrated that PSF1 is highly expressed in proliferating HSCs and progenitors.

Pool size of HSCs/HPCs is decreased in *PSF1*$^{+/-}$ old mice

To investigate how haploinsufficiency of *PSF1* affects hematopoiesis, we analyzed the BM of *PSF1*$^{+/-}$ mice.[18] Although no significant differences were found in KSL cells (Figure 2A) and mature cells populations (data not shown) between wild-type and *PSF1*$^{+/-}$ at 8 weeks of age, the relative number of KSL cells was approximately 2-fold lower in one year-old mice compared with wild-type littermates (Figure 2B). In addition, the population of CD34$^-$ KSL cells (LT-HSCs), CD34$^+$ KSL cells (KSL: ST-HSCs),

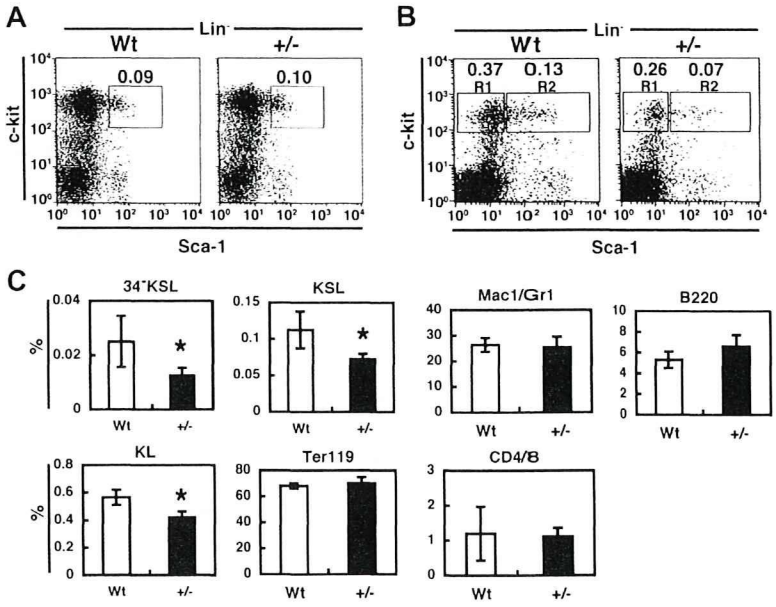

Figure 2. Haploinsufficiency of *PSF1* for hematopoiesis. (A,B) Cells of KSL populations in the BM from 8-week-old mice (A) and 1-year-old mice (B) were analyzed. Percentage of each fraction indicated by box was represented. R1 and R2 in panel B indicates fraction from c-kit$^+$Sca-1$^-$Lin$^-$ cells and c-kit$^+$Sca-1$^+$Lin$^-$ cells, respectively. (C) Quantitative evaluation in percentage of each fraction among all BM cells of 1-year-old wild-type (Wt) or *PSF1*$^{+/-}$ (+/−) mice as indicated. Mac-1/Gr-1 (myeloid), B220 (B cells), CD4/CD8 (T cells), or TER119 (erythroid). HSCs populations were studied in a CD34$^-$ KSL cell population. Populations of KSL (c-kit$^+$Sca-1$^+$Lin$^-$ cells) and KL (c-kit$^+$Sca-1$^-$Lin$^-$ cells) were also evaluated. *$P < .05$.

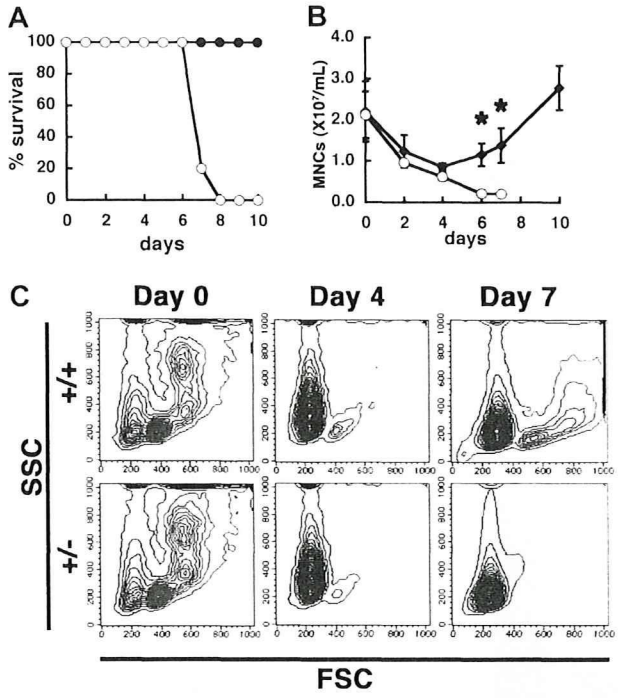

Figure 3. Hypersensitivity of *PSF1*$^{+/-}$ mice to 5-FU. (A) Survival curves after 5-FU injection. ○ indicate *PSF1*$^{+/-}$ 8-week-old mice (n = 10); and ●, wild-type 8-week-old mice (n = 10). (B) Number of mononuclear cells in the peripheral blood of wild-type (●) and *PSF1*$^{+/-}$ (○) mice over time after 5-FU injection. 5-FU was injected into 8-week-old mice on day 0. Means plus or minus SEM are shown (n = 10). *$P < .05$ vs those in PSF1$^{+/-}$ mice on days 2, 4, 6, 8, and 10 after BM ablation with 5-FU. (C) Kinetics of BM cells after 5-FU injection. +/+ indicates wild-type mice; and +/−, *PSF1*$^{+/-}$ mice. Results of FACS analysis are shown. SSC indicates side-scattered light; and FSC, forward-scattered light. Blue represents RBC; and red, leukocytes.

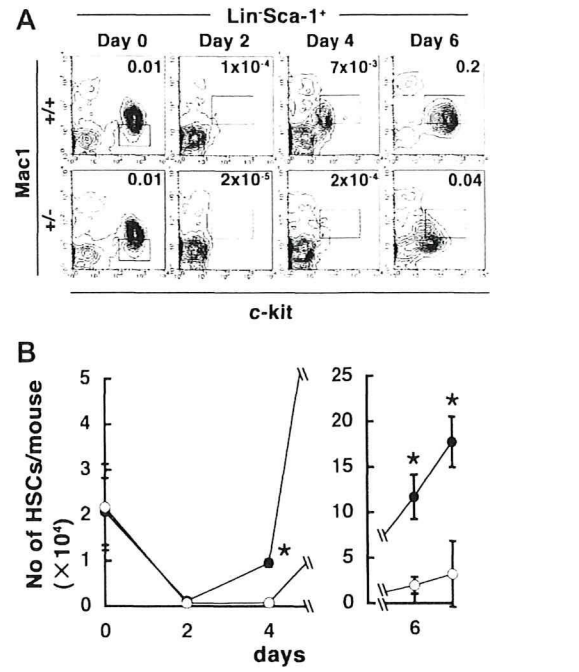

Figure 4. Both alleles of *PSF1* are required for acute reconstitution after BM ablation. (A) Time course of c-kit and Mac-1 expression in Lin$^-$Sca-1$^+$ cells during BM reconstitution after 5-FU injection (+/+, 8-week-old wild-type mice; +/−, 8-week-old *PSF1*$^{+/-}$ mice). Results of FACS analysis are shown. Boxes indicate HSC-containing populations. Percentage of all BM cells corresponding to HSC population indicated by the box is shown in the right corner of each figure. (B) Total number of KSL cells derived from the femurs and tibias of wild-type (●) and *PSF1*$^{+/-}$ mice (○) on the indicated days before (day 0) and after 5-FU injection as described in panel A. *$P < .05$ versus that in *PSF1*$^{+/-}$ mice on the respective day.

and c-kit$^+$Sca-1$^-$Lin$^-$ (KL) were significantly decreased in *PSF1*$^{+/-}$ mice (Figure 2C). The relative cell number of each type of mature HC such as myeloid cells (Mac1/Gr-1$^+$ cells), T cells (CD4/CD8 cells), B cells (B220$^+$), or erythroid cells (TER119$^+$) of the *PSF1*$^{+/-}$ BM was similar to that of the wild-type BM (Figure 2C). These data suggested that both alleles of *PSF1* gene are essential for maintenance of the proper pool size of HSCs or HPCs throughout life.

PSF1$^{+/-}$ mice show hypersensitivity for fluorouracil in the BM

Next, we ablated the BM by 5-FU injection, which kills cycling HSCs/HPCs and forces dormant HSCs into cycle, and studied the ability of *PSF1*$^{+/-}$ mice to reconstitute BM hematopoiesis and analyzed the effect of haploinsufficiency of *PSF1* on HSCs and HPCs (Figure 3A). Although the LD_{50} of 5-FU is 350 mg/kg in normal mice,[28] the *PSF1*$^{+/-}$ mice died within 8 days after a single injection with a lower dose 5-FU (150 mg/kg), whereas wild-type mice did not die with this treatment. On 5-FU injection in *PSF1*$^{+/-}$ mice, the number of peripheral leukocytes decreased precipitously over 7 days; however, in wild-type mice, the number of peripheral leukocytes decreased over 4 days and then it began to increase by day 6 (Figure 3B). After 5-FU injection, the forward scatter$^{dull/high}$ population, which includes lymphocytes, granulocytes, and monocytes, were reconstituted in the BM of wild-type mice after approximately day 7; however, such reconstitution was not observed in the BM of *PSF1*$^{+/-}$ mice (Figure 3C red-colored population). We also calculated the number of peripheral red blood cells and platelets; however, no significant differences were found between *PSF1*$^{+/+}$ and *PSF1*$^{+/-}$ mice in normal and acute phase (data not shown).

PSF1 is essential for HSC proliferation after 5-FU treatment

Before 5-FU injection, there were no obvious differences in the numbers of HSCs and HPCs in the BM between 8-week-old wild-type and *PSF1*$^{+/-}$ mice (Figures 2A, 4A). 5-FU injection induces HSCs into cycle, and it was reported that these cycling HSCs weakly express Mac-1.[26,29] We therefore studied whether 5-FU injection promotes the proliferation of Mac-1^{lo}–expressing HSCs. Before 5-FU injection, the number of HSC population designated as Mac-1$^-$ KSL was not significantly different between wild-type and *PSF1*$^{+/-}$ mice as shown in Figure 2A (see also Figure 4A,B). After 5-FU injection, the KSL cell population decreased in both wild-type and *PSF1*$^{+/-}$ mice during the first few days (Figure 4A). Four to 6 days after 5-FU injection, the population of cycling Mac-1^{lo}–KSL cells increased dramatically in wild-type mice, whereas very few of the KSL cells except for the Mac-1^{lo}–KSL population appeared in the *PSF1*$^{+/-}$ mice (Figure 4A). Because of this delay of recovery, the absolute number of HSCs in the BM was approximately 5.9-fold lower in *PSF1*$^{+/-}$ mice compared with that in wild-type mice at 6 days after 5-FU treatment (Figure 4B).

Loss of PSF1 leads to delayed HSC proliferation in the acute phase after BM ablation

Because it has been reported that the percentage of proliferating HSCs reaches a maximum on approximately day 6 in normal mice,[29] we sorted the total population of HSCs (KSL–Mac-1$^{-/lo}$) and HPCs (Lin$^-$Sca-1$^-$c-kit$^+$Mac-1$^{-/lo}$) on day 6 after 5-FU

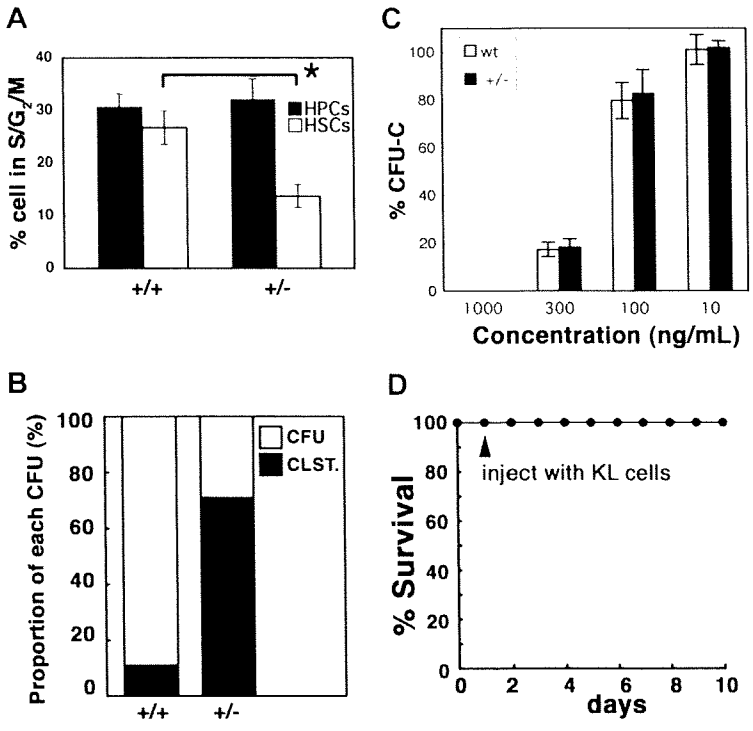

Figure 5. Loss of PSF1 leads to delay of HSC proliferation in the acute phase. (A) Percentage of KSL cells or HPCs ($Lin^-c\text{-}kit^+Sca\text{-}1^-$) in the $S/G_2/M$ phase among the total number of HSCs or HPCs, respectively, on day 6 after 5-FU injection as described in Figure 4A. ■ indicates HPCs; □, KSL cells. Mean values plus or minus SEM are shown (n = 5). *$P < .05$. (B) CFU-c assay using KSL cells obtained from mice on day 6 after 5-FU injection. +/+ indicates wild-type mice; and +/−, $PSF1^{+/-}$ mice. ■ indicates CFU cluster (CLST; containing < 30 cells); □, CFU-C (CFU; containing > 30 cells). (C) Comparison between wild-type and $PSF1^{+/-}$ KSL cells for sensitivity to 5-FU toxicity. Sorted KSL cells from the BM of 8-week-old mice were seeded in semisolid medium with indicated concentration of 5-FU, and total CFU-C number was counted after 10 days of culturing. Results are expressed as a percentage compared with control condition (100%). (D) Rescue experiments. $PSF1^{+/-}$ mice were injected with 5-FU on day 0. One day after 5-FU injection (▲), $Lin^-CD45^+c\text{-}kit^+$ cells (KL cells; 5×10^4/mice) that had been derived from wild-type BM were injected into $PSF1^{+/-}$ mice (n = 5).

injection and analyzed the cell cycle of those HSCs and HPCs. The cells were analyzed for DNA content by PI staining (Figure 5A). The percentage of HSCs in the $S/G_2/M$ phase was approximately 50% lower in $PSF1^{+/-}$ mice than those in wild-type mice, whereas the percentage of HPCs in the $S/G_2/M$ phase was not significantly different between $PSF1^{+/-}$ and wild-type mice. These data suggest that both alleles of *PSF1* are essential for acute BM reconstitution.

When HSCs are cultured in semisolid media, they divide and generate large colonies, including mature HCs. If *PSF1* haploinsufficiency leads to cell death in HSCs, HSCs cannot form colonies in vitro. Therefore, next we investigated the in vitro colony-forming capacity of HSCs ($KSL\text{-}Mac\text{-}1^{-/lo}$) that had been obtained on day 6 after 5-FU injection by cell sorting (Figure 5B). The HSCs from $PSF1^{+/+}$ and $PSF1^{+/-}$ mice formed the same total numbers of colonies and clusters (data not shown); however, the HSCs from $PSF1^{+/-}$ mice formed a markedly higher number of CFU clusters (> 30 cells) compared with $PSF1^{+/+}$ cells. In the case of HSCs derived from wild-type mice, approximately 89% of all colonies were large colonies; however, approximately 71% of colonies generated by HSCs from $PSF1^{+/-}$ mice were small colonies. To determine whether haploinsufficiency of *PSF1* simply induced cell death resulting in reduced colony size in CFU-c assay, we examined the number of apoptotic cells in the colony-forming cell population by staining with anti–annexin V antibodies (Table 1). No significant differences were found in the apoptotic cells with respect to Lin^-Kit^+, Lin^-Sca1^+, and Lin^- population between cells from CFU-c derived from $PSF1^{+/+}$ and $PSF1^{+/-}$ HSCs. These data suggested that the decreased colony size in $PSF1^{+/-}$ CFU-c is not induced by activation of DNA damage checkpoint and cell death. These results indicated that $PSF1^{+/-}$ HSCs may not easily divide into daughter cells committed to a program of differentiation, but haploinsufficiency did not induce cell death. Furthermore, to test the possibility that $PSF1^{+/-}$ HSCs are simply more sensitive to 5-FU toxicity, KSL cells were sorted from BM of wild-type or $PSF1^{+/-}$ mice and seeded onto semisolid medium in the presence or absence of 5-FU. Figure 5C illustrates the effect of exposure to various concentrations of 5-FU on colony-forming activity of KSL cells. KSL cells survived and those from wild-type and $PSF1^{+/-}$ formed comparable number of colonies, suggesting that deletion of one *PSF1* allele of HSCs does not cause hypersensitivity for 5-FU. To support this interpretation, BM of wild-type or $PSF1^{+/-}$ mice was collected after 1 day of 5-FU treatment and transplanted into lethally irradiated recipient mice together with untreated normal cells as competitor. After 4 weeks of transplantation, donor contribution was determined by FACS. The percentage of contributed cells (chimerism) was 56 plus or minus 12 and 24 plus or minus 14 in recipients, which were transplanted with wild-type or $PSF1^{+/-}$ BM cells, respectively, although the contribution of $PSF1^{+/-}$-derived HSCs in recipient mice was slightly less. These data suggested that deletion of one *PSF1* allele of HSCs does not cause hypersensitivity for 5-FU. Moreover, transplantation of HSCs and HPCs that had been obtained from wild-type mice completely rescued the lethality of 5-FU in $PSF1^{+/-}$ mice (Figure 5D). These data suggest that the defect in acute reconstitution of the BM in $PSF1^{+/-}$ mice is not caused by disruption of the BM microenvironment in these mice.

Table 1. Percentage of apoptotic cells among CFU-c cell population

	Genotype	
Marker	$PSF1^{+/+}$	$PSF1^{+/-}$
Lin^-Kit^+	39 ± 33	36 ± 29
Lin^-Sca1^+	3.6 ± 2.3	2.6 ± 1.6
Lin^-	2.2 ± 1.1	1.8 ± 1.4

It was reported that PSF1 is essential for DNA replication in yeast.[14-17] This observation raises the possibility that haploinsufficiency of *PSF1* leads to abnormal DNA replication, activation of DNA damage checkpoint, S-phase arrest, and cell death in mice. To evaluate this possibility, apoptotic cells were quantified by FACS analysis after staining with annexin V in 5-FU–treated or untreated BM cells (Table 2). In $PSF1^{+/-}$ BM cells, apoptotic cells from Lin^-, Lin^-Kit^+, or $Lin^-Kit^+Sca^+$ cell populations were slightly